Monday Posters

Poster-Mo01

Easy-plane ferroborates. Magnetopiezoelectric effects

T.N.Gaydamak[1], V.D. Fil[1], I. A Gudim[2]

[1]*B.Verkin Institute for Low Temperature Physics and Engineering of NAS of Ukraine,47 Nauky Ave., Kharkiv, 61103, Ukraine*

[2]*L.V. Kirensky Institute for Physics, Siberian Branch of the Russian Academy of Sciences,660036, Krasnoyarsk, Russia*

Rare-earth borates with formula $RFe_3(BO_3)_4$ (R = Y; La-Nd; Sm-Er) are popular object of study because they the materials which combine magnetically ordered and ferroelectric media properties. This is why ferroborates belong to the family of multiferroics[1].

Since ferroborates belong to noncentrosymmetric class 32, the direct piezoelectric effect (PE) is allowed in these crystals. We have investigated the piezoelectric properties of $SmFe_3(BO_3)_4$ and $NdFe_3(BO_3)_4$ single crystals using the acoustic method [2]. It was found that in those compounds, the value of the piezoelectric modulus e11 in the paraelectric phase (≈ 1.4 C/m^2) was almost an order of magnitude higher than that of the α - quartz, and, therefore, such compounds may be recommended for technical applications.

In addition to the above-mentioned direct PE in multiferroics the indirect PE may exist. It consists in the joint action of the magnetoelastic and magnetoelectric mechanisms. Due to magnetoelasticity deformation changes the state of magnetic variables and through the magnetoelectric coupling excites the electric field (and vice versa). This effect was first discovered in samarium ferroborate [3].

In $NdFe_3(BO_3)_4$ direct renormalization of the piezoelectric interaction in a magnetically ordered phase is observed [4].

[1] A.M. Kadomtseva,Yu. F. Popov, G. P.Vorob'ev, and all. Low Temp. Phys. 36, 511(2010).

[2] T.N.Gaydamak, I.A.Gudim, G.A.Zvyagina, I.V.Bilych, N.G.Burma, K.R.Zhekov, V.D.Fil, Low Temp. Phys. 41, 614 (2015).

[3] T.N.Gaydamak, I.A.Gudim, G.A.Zvyagina, I.V.Bilych, N.G.Burma, K.R.Zhekov, V.D.Fil, Phys. Rev. B 92, 214428 (2015).

[4] I. V. Bilych, K. R. Zhekov, T. N. Gaydamak, I. A. Gudim, G. A. Zvyagina, and V. D. Fil , Low Temp. Phys. 42, 1112 (2016).

Poster-Mo02

Optical and Magnetic properties of Eu Doped Tin Chalcogenides

Samih Isber[1] and Xavier Gratens[2]

[1]*American University of Beirut, Physics Department, Bliss Street, P.O. Box 11-0236, Beirut, Lebanon*

[2]*Instituto de Física, Universidade de São Paulo, Caixa Postal 66.318, 05315-970, São Paulo, Brazil*

In the present study, we investigate the magnetic and optical properties of Europium doped IV-VI tin chalcogenides (SnSe and SnS). Unlike other studied rare-earth doped IV-VI materials, SnSe and SnS crystallize in a double layer like orthorhombic crystal. The Eu ions have different environment, reflected by the low site symmetry, as well as a different number of nearest neighbors. The investigation is based on Infrared optical absorption spectra, low temperature magnetization and Electron Paramagnetic Resonance (EPR) measurements. Q-Band (34 GHz) EPR measurements showed that the site symmetry of Eu^{2+} at 4.2 K is orthorhombic and the average Landé factor was determined to be g =1.99 ± 0.01 and 1.97 ± 0.01, for Eu^{2+} in SnSe and SnS, respectively. The Band Gap energy of both samples $Sn_{1-x}Eu_xSe$ and $Sn_{1-x}Eu_xS$ (x ~ 0.03) were determined from the optical absorption spectra and found to be 0.90 ± 0.01 eV and 1.12 ± 0.01 eV, respectively. For both samples, the exchange-coupling between nearest-neighbors (NN) Eu^{2+} ions was estimated from magnetization and magnetic susceptibility measurements using a model that takes into account the magnetic contributions of single ions, pairs and triplets.

Poster-Mo03

Enhanced Structural and Magnetic Properties of Carbon-Assisted ZnO Nanorod Arrays on (100) Si

Im Taek Yoon,[1] Hak Dong Cho,[1] Dmitry V. Roshchupkin,[2] Sejoon Lee,[3] Yoochul Yang,[3]

[1]*Quantum Functional Semiconductor Research Center, Dongguk University, Seoul, 100-715, Republic of Korea*

[2]*Institute of Microelectronics Technology and High-Purity Materials, Russian Academy of Sciences, Chernogolovka 142432, Russian Federation*

[3]*Department of Physics and Semiconductor Science, Dongguk University, Seoul 100-715, Korea*

ZnO is a particularly promising material for optoelectronic devices on a miniaturized scale because it has a bandgap of 3.37 eV at room temperature, a large exciton binding energy of 60 meV and a large surface-to-volume ratio. We have fabricated as-grown ZnO nanorods (NRs) and carbon-assisted NRs arrays on semi-insulating (100)-oriented Si substrates. we used a vapor-phase transport (VPT) method of using thin carbon layer to assist the nucleation of vertically aligned single crystalline ZnO NRs on Si substrates. The carbon layer with the thickness of around 9 nm was deposited using low pressure chemical vapor deposition (LPCVD) method on Si substrate before the ZnO NRs growth using VPT method. The major purpose of a carbon-assisted process is that it avoids undesired contamination from foreign metal atoms used as catalysts and not only to facilitate the nucleation of ZnO nuclei but also to decrease the lattice mismatch between the Si substrate and the ZnO NRs. The carbon-assisted process also avoids undesired SiO2 layer on Si substrate to limit optoelectronic application such as field emission display, et al. We compared the structural and magnetic properties of them. HRTEM (High Resolution Transmission Microscopy), Field emission scanning electron microscopy (FESEM), X-ray diffraction (XRD), Energy dispersive X-ray (EDS) revealed that the as-grown ZnO NRs and carbon-assisted ZnO NRs were single crystals with a hexagonal wurtzite structure, and grew with a c-axis orientation perpendicular to the Si substrate. These measurements show that the carbon-assisted ZnO NRs were better synthesized vertically on a Si substrate compared to the as-grown ZnO NRs. In addition, we aim to probe the role of defects on magnetic properties of the carbon-assisted ZnO NRs compared to the as-grown ZnO NRs. Therefore, we investigate the structural and magnetic properties of the carbon-assisted ZnO NR array compared to the sample not assisted with carbon. Superconducting Quantum Interference Device (SQUID) and X-ray photoelectron spectroscopy (XPS) measurements showed that defect concentration of the carbon-assisted ZnO NRs was remarkably reduced compared to the as-grown ZnO NRs. The reduced defect concentration of the carbon-assisted ZnO demonstrates the possible improvement in the performance of photovoltaic nanodevices based on ZnO like materials. This method can be applied to the fabrication of well-aligned ZnO nanorod used widely in optoelectronic devices.

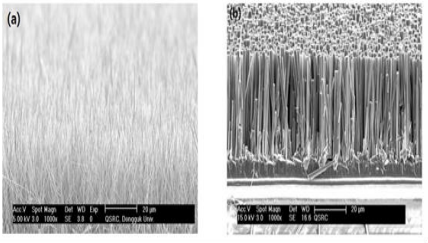

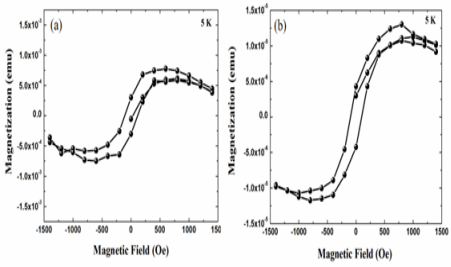

FIG.1. (a) Cross-sectional SEM image of the as-grown ZnO nanorods and (b) carbon-assisted ZnO nanorods on Si substrate (a) scale bar: 20 μm (b) scale bar: 20 μm

FIG. 2. Ferromagnetic hysteresis loop of the (a) as-grown ZnO nanorods and (b) carbon-assisted ZnO nanorods measured by SQUID magnetometer at 5 K. The solid line serves as a visual guide.

[1]S. Xie, X. Lu, T. Zhai, W. Li, M. Yu, C. Liang, and Y. Tong, J. Mater. Chem. 22, 14272, (2012).
[2]X. Yang, A. Wolcott, G. Wang, A. Sobo, R. C. Fitzmorris, F. Qian, J. Z. Zhang, and Y. Li, Nano Lett. 9, 2331, (2009).
[3]K. K. Naik, R. Khare, D. Chakravarty, M. A. More, R. Thapa, D. J. Late, and C. S. Rou, Appl. Phys. Lett. 105, 233101, (2014).
[4]F. J. Sheini, K. R. Patil, D. S. Joag, M. A. More, Appl. Surf. Sci. 257, 8366, (2011).
[5]S. Kumar, Y.J. Kim, B.H. Koo, S. Gautam, K.H. Chae, Ravi Kumar, and C.G. Lee, Mater. Lett. 63, 194, (2009).
[6]B. Panigrahy, M. Aslam, D. S. Misra, M. Ghosh, and D. Bahadur, Adv. Func. Mater. 2010, 1, (2010).

Poster-Mo04

Multi-carrier transport in a concentrated ferromagnetic semiconductor

P.A.E Murgatroyd,[1] T.D. Veal,[1] and J. Alaria[1]

[1] *Department of Physics, University of Liverpool, Liverpool, United Kingdom*

A major focus within the field of spintronics is the understanding of the spin-dependent transport arising from correlation between free carriers and magnetic exchange interactions. Extensive research has been carried out upon europium chalcogenides and dilute magnetic semiconductors as the primary examples of ferromagnetic semiconductors. However both classes of material have inherent properties that are detrimental to such studies. Europium chalcogenides, despite being concentrated ferromagnetic semiconductors, present poor mobilities due to **d-f** scattering mechanisms and require studying within a magnetic polaron framework. The dilute magnetic semiconductors, in despite of their valence band **p-d** mechanisms, often present degenerate characteristics with the introduction of magnetic impurities being destructive to the semiconducting properties of the host.

The chalcochromite spinels are a family of material in which a true ferromagnetic semiconductor may reside. $HgCr_2Se_4$ is a member of this family that has been sporadically studied over the past 50 years but has yet to have its properties definitively characterized, and is the material of interest within this study. $HgCr_2Se_4$ is well reported as being a semiconductor within the paramagnetic regime with a band gap of 0.8 eV. However, the literature diverges as the system transitions into the ferromagnetic regime with many alternative theories reported.

Magneto-transport measurements have been carried out on as-grown $HgCr_2Se_4$ and Hg-annealed $HgCr_2Se_4$ single crystals in magnetic fields up to 14T between 2K and 300K, in Van der Pauw geometry. Symmetrization of the resistance into magnetoresistance (MR) and Hall components has been performed, with both components simultaneously fitted using a modified multi-carrier conductivity tensor. Resistance as a function of temperature at fixed fields has also been measured for both systems.

Transport studies for the as-grown system have revealed four distinct transport regimes: namely an activated semiconducting regime between 2K and 10K; an **s-d** scattering regime between 10K and 60K; a magnetically bound polaron regime between 60K and 150K; and an activated semiconducting regime at higher temperatures (figure 1). The simultaneous fitting of MR and Hall data requires both electrons and holes to be active in transport between 2K and 10K with carrier densities of the order 10^{16} cm^{-3} and 10^{15} cm^{-3} respectively and mobilites of the order 180 $cm^2V^{-1}s^{-1}$ and 350 $cm^2V^{-1}s^{-1}$ respectively.

Transport studies for the Hg annealed sample show a degenerate semiconducting regime. Below the Curie temperature the simultaneous fitting of the longitudinal and transverse MR leads to light (0.08 m_0) and heavy (0.4 m_0) electrons with carrier densities of 10^{18} cm^{-3} and 10^{17} cm^{-3} respectively. Above the Curie temperature, only one type of carrier is observed and the inclusion of paramagnetic scattering is required to describe the magneto-transport properties. The temperature dependence of the mobility shows that it is controlled by magnetic fluctuations and indicates that this compound has the characteristic of a conduction band **s-d** scattering magnetic semiconductor.

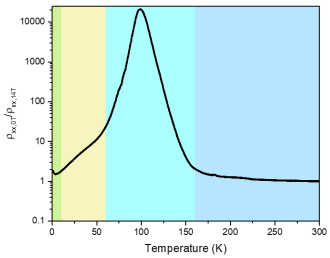

FIG. 1. *The ratio of magnetoresistance between 0T and 14T as a function of temperature for as-grown $HgCr_2Se_4$ demonstrating four distinct transport regimes; an activated semiconducting regime between 2K and 10K; an* **s-d** *scattering regime between 10K and 60K; a magnetically bound polaron regime between 60K and 150K; and an activated semiconducting regime at higher temperatures*

Poster-Mo05

Exciton-light coupling in quantum wells in magnetic field

P. S. Grigoryev,[1] Yu. P. Efimov,[2] S. A. Eliseev,[2] D. K. Loginov,[2]
V. A. Lovtcius,[2] P. Yu. Shapochkin,[2] and I. V. Ignatiev[1]

[1] *Spin Optics Laboratory, St. Petersburg State University, Ulyanovskaya 1, 198504 St. Petersburg, Russia*

[2] *Department of Physics, St. Petersburg State University, Ulyanovskaya 1, 198504 St. Petersburg, Russia*

The high quality of heterostructures grown by MBE technology allows one to experimentally study variety of the fine magnetic-field induced effects for excitons [1,2]. Theoretical modeling of the effects helps in extracting information about the exciton energy structure and the exciton-light coupling in quantum wells (QWs) [2,3]

In this report, we present results of experimental study of the two magnetic-field induced effects for excitons in the GaAs/(Al,Ga)As and (In,Ga)As/GaAs QWs. The first effect is a modification of the exciton dispersion when a magnetic field transverse to the growth axis is applied to the structure. The study of reflectance spectra is performed for a wide ($L = 240$ nm) GaAs/(Al,Ga)As QW in magnetic fields $B = 0 \div 3$ T. Multiple resonances observed in the spectra are attributed to the quantum-confined exciton states in the QW. Their analysis allows one to restore the exciton dispersion in the QW material. The energy distance between the resonances decreases with the magnetic field that indicates the dispersion modification. It can be described as a parabolic-like increase of the effective exciton mass up to 30 % at $B = 3$ T.

Longitudinal magnetic field produces another remarkable effect. Magnetic field increases exciton-light coupling. As seen in reflectance spectra shown in Fig. 1 for heterostructure with 95-nm (In,Ga)As/GaAs QW. There are several exciton resonances observed as peaks or dips in the spectra. Intensities of the resonances increase with the magnetic field. This effect may be quantitatively analyzed using the reflectance spectra modeling [4]. The inset in Fig. 1 shows that the exciton-light coupling constant, Γ_0, obtained for the lowest exciton transition by the modeling monotonically increases and becomes twice larger in the magnetic field $B = 6$ T.

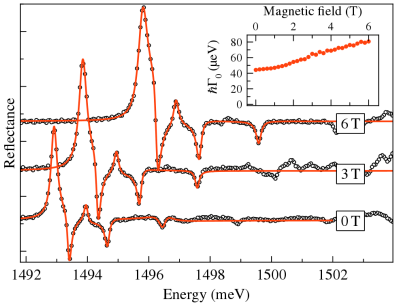

FIG. 1. *Exciton resonances in reflectance spectra of a structure with the 95-nm (In,Ga)As/GaAs QW in the longitudinal magnetic field. Inset shows the increase of the radiative decay rate (in energy units) for the lowest exciton transition.*

The authors acknowledge Saint-Petersburg State University for a research grant 11.34.2.2012. The studied heterostructure was grown in the resource center Nanophotonics of St. Petersburg State University.

[1] J. J. Davies and D. Wolverson, V. P. Kochereshko *et al.*, "Motional Enhancement of Exciton Magnetic Moments in Zinc-Blende Semiconductors", Phys. Rev. Lett. **97**, 187403 (2006).

[2] P. S. Grigoryev, O. A. Yugov, S. A. Eliseev *et al.*, "Inversion of Zeeman splitting of exciton states in InGaAs quantum wells", Phys. Rev. B **93**, 205425 (2016)

[3] S. Yu. Bodnar, P. S. Grigoryev, D. K. Loginov, *et al.*, "Exciton mass increase in a GaAs/AlGaAs quantum well in a transverse magnetic field", Phys. Rev. B **95**, 195311 (2017).

[4] E. S. Khramtsov, P. A. Belov, P. S. Grigoryev *et al.*, "Radiative decay rate of excitons in square quantum wells: Microscopic modeling and experiment", J. Appl. Phys. **119**, 184301 (2016)

Poster-Mo06

Two-dimensional biexcitons and cavity polaritons in the strong perpendicular magnetic field

S.A. Moskalenko,[1] P.I. Khadzhi,[1] I.V. Podlesny,[1] E.V. Dumanov,[1] M.A. Liberman,[2] B.V. Novikov,[1] I.A. Zubac[1]

[1]*Institute of Applied Physics of the Academy of Sciences of Moldova, Academic str. 5, Chisinau, MD-2028 Republic of Moldova*

[2]*Nordic Institute for Theoretical Physics (NORDITA) KTH and Stockholm University, Roslagstullsbacken 23, Stockholm, SE-106 91 Sweden*

[3]*Department of Solid State Physics, St. Petersburg State University, Institute of Physics, 1, Ulyanovskaya Street, Petrodvorets, 198504 St. Petersburg, Russia*

The possible existence of bound states of the interacting two-dimensional (2D) magnetoexcitons with different spin structures in the lowest Landau levels (LLLs) approximation was investigated using the Landau gauge description. The magnetoexcitons taking part in the formation of the bound state with resultant wave vector $\vec{k}=0$ have opposite in-plane wave vectors $\vec{k}$ and $-\vec{k}$ and look as two electric dipoles with the arms oriented in-plane perpendicularly to the corresponding wave vectors. The length of the arms equals to $d=kl_0^2$, where l_0 is the magnetic length. The bound state of two antiparallel dipoles moving with equal but antiparallel wave vectors in any direction of the plane with equal probability is characterized by the variational wave function of the relative motion $\varphi_n(\vec{k})$ depending on the modulus $|\vec{k}|$. The magnetoexcitons are composed of electrons and holes situated on the LLLs with cyclotron energies greater than the binding energies of the 2D Wannier-Mott exciton, and interact through the Coulomb interactions of their constituents.

The spins of the electrons and the effective spins of two holes forming the bound states were combining separately in the symmetric or in the antisymmetric forms ($\uparrow\downarrow+\eta\downarrow\uparrow$) with the same parameter $\eta=\pm1$ for electrons and holes. Two types of wave functions, one with singlet electron and singlet hole structure and another one with triplet electron and triplet hole structure were used, leading to completely different bound states. The mixt states of the type singlet electrons and triplet hole or vice versa do not exist due to the hidden symmetry of the electron and hole in the lowest Landau levels in the Landau gauge description. Because the projections of the both spinor states with $\eta=\pm1$ are equal to zero, the effect of the Zeeman splitting vanishes. The para and ortho magnetoexciton states up till now were not investigated and the splitting of their energy levels is unknown at present time.

In the case of the variational wave function $\varphi_2(k)=(8\alpha^3)^{1/2}k^2l_0^2e^{-\alpha k^2l_0^2}$ the maximum density of the magnetoexcitons in the momentum space representation is concentrated on the in-plane ring with the radius $k_r=1/(l_0\sqrt{\alpha})$. In the LLLs approximation, when the influence of the excited Landau levels (ELLs), as well as of the Rashba spin-orbit coupling (RSOC) are neglected, the stable bound states of the bimagnetoexciton molecule do not exist for both spin orientations. Instead of them, a deep metastable bound state with the activation barrier comparable with double ionization potentials $2I_l$ of the magnetoexciton with $\vec{k}=0$ was revealed in the case $\eta=1$ and $\alpha=0.5$. In the case $\eta=-1$ and $\alpha=3.4$ only a shallow metastable bound state can appear. In the case of the variational wave function $\varphi_0(k)=(4\alpha)^{1/2}e^{-\alpha k^2l_0^2}$ all the bound states are unstable and the molecule bimagnetoexciton cannot be formed in the LLLs approximation.

The energy spectrum of the two-dimensional cavity magnetoexciton-polaritons was investigated. The effective polariton mass on the lower polariton branch, the Rabi frequency and the corresponding Hopfield coefficients were determined in dependence on the magnetic field strength and on the Rashba spin-orbit coupling parameters.

Supplementary to the Ref. [1], new results concerning the Zeeman splitting effects at different values of the electron and hole g-factors were investigated.

[1] Sveatoslav A. Moskalenko, Igor V. Podlesny, Evgheni V. Dumanov, Michael A. Liberman, and Boris V. Novikov, Journal of Nanophotonics, 10(3), 036006 (2016), http://dx.doi.org/10.1117/1.JNP.10.036006

Poster-Mo07

Halperin 331 state of the FQH system of the n=0 Landau band of graphene

Koji Kudo[1] and Yasuhiro Hatsugai[1]

[1] *Graduate School of Pure and Applied Sciences, University of Tsukuba, Tsukuba, Japan*

The internal degrees of freedom, such as spin or layer index, generate further diversity in the fractional quantum Hall (FQH) phases. The Halperin 331 state of the bilayer FQH system at $\nu = 1/2$ is the typical example. The graphene FQH system is also such an example of the multi-component FQH phases. Using 2 Landau levels (LL) of massless Dirac fermions at K and K' points, FQH effects for $n = 0$ LL of graphene have been discussed with SU(2) invariance [1,2]. Here, we discuss the FQH states of graphene by fully taking account of the honeycomb lattice structure. Short range electron-electron interaction of the nearest-neighbor (NN) and next nearest-neighbor (NNN) is considered by constructing a pseudopotential projected into the $n = 0$ Landau band of honeycomb lattice [3]. Further, the Chern number matrix [4] defined by twisting the boundary condition is evaluated numerically.

We have put a focus on the $\nu = 1/2$ state of the $n = 0$ Landau band. Topological phase transition associated with different topological degeneracy occurs by change V_2/V_1 (Fig.1 (a)), where $V_{1(2)}$ is the strength of the NN (NNN) interaction. Due to the chiral symmetry of the honeycomb lattice, z-component of the pseudospin is conserved as a total chirality. Since the total pseudospin is not conserved, the SU(2) symmetry is absent. This is similar to the conventional bilayer FQH system, where the NN and NNN interactions on honeycomb lattice correspond to the interlayer and intralayer ones respectively. Also, the Berry connection of the m-fold degenerated ground state multiplet $\Phi = (|G_1\rangle, \cdots, |G_m\rangle)$ is defined as $\boldsymbol{A}_{\alpha\beta} = \Phi^\dagger d\Phi$, where $\alpha, \beta = \pm$, $d = d\theta^x_\alpha \frac{\partial}{\partial\theta^x_\alpha} + d\theta^y_\beta \frac{\partial}{\partial\theta^y_\beta}$, and $\theta^\mu_\pm$ specifies the twisted boundary condition in μ-direction and the chirality $\pm$. Then, the Chern number matrix is defined as $\boldsymbol{C} = \begin{pmatrix} C_{++} & C_{+-} \\ C_{-+} & C_{--} \end{pmatrix}$ and calculated by using the method in Ref.[5], where $C_{\alpha\beta} = \frac{1}{2\pi i}\int_{T^2} \mathrm{Tr}\boldsymbol{F}_{\alpha\beta}$ and $\boldsymbol{F}_{\alpha\beta} = d\boldsymbol{A}_{\alpha\beta} + \boldsymbol{A}^2_{\alpha\beta}$. In the Fig.1 (b), the many-body spectrum for $V_2 = V_1$ for the total chirality =0 is plotted as a function of θ^x_+. The eight low energy states are entangled each other and do not mix with excited states. The numerically obtained Chern number matrix defined by this multiplet is consistently discussed by the analogue of the Halperin 331 state [6].

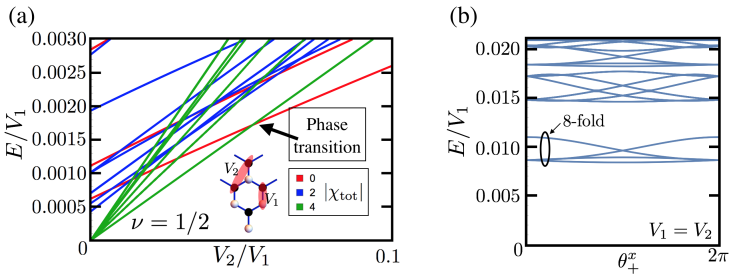

FIG. 1. *(a) Many-body spectrum as a function of V_2/V_1 is shown. The total chirality is expressed by the color of the lines. (b) Chirality-unpolarized many-body spectrum as a function of the twisted boundary θ^x_+ for $V_2 = V_1$. The numerically obtained Chern number matrix indicates that the 8-fold ground state multiplet is consistent with the Halperin 331 state.*

[1] V. M. Apalkov, and T. Chakraborty, Phys. Rev. Lett. **97**, 126801 (2006).

[2] C. Töke, P.E. Lammert, V.H. Crespi, and J. K. Jain, Phys. Rev. B **74**, 235417 (2006).

[3] Y. Hamamoto, H. Aoki, and Y. Hatsugai, Phys. Rev. B **86**, 205424 (2012).

[4] T.-S. Zeng, W. Zhu, and D. N. Sheng, Phys. Rev. B **95**, 125134 (2017).

[5] Koji Kudo, Toshikaze Kariyado, and Yasuhiro Hatsugai, J. Phys. Soc. Jpn. **86**, 103701 (2017)

[6] Koji Kudo, and Yasuhiro Hatsugai, in preparation.

Quantum oscillations in Dirac Cd_3As_2 and nodal line ZrSiS semimetals

F. Orbanić[1], M. Novak[1], A. McCollam[2], L. Tang[2], I. Kokanović[1]

[1] Department of Physics, Faculty of Science, University of Zagreb, Zagreb, Croatia
[2] High Field Magnet Laboratory, Radbound University, Nijmegen, the Netherlands

Dirac semimetals are three-dimensional phases of matter with gapless electronic excitations that are protected by topology and symmetry. They possess linear band dispersion around symmetry-protected crossing points of the valence and conduction bands (Dirac points). Because of the topology of the energy bands and the existence of Dirac points these materials possess fundamentally very interesting transport and magnetic properties. Cd_3As_2 is predicted to be a symmetry-protected topological semimetal with a single pair of three-dimensional (3D) Dirac points in the bulk and unusual Fermi arcs on the surfaces. It can be driven into a topological insulator and a Weyl semimetal state by symmetry breaking. The nodal loop ZrSiS semimetal is regarded as a promising new material with a very wide energy window (0-2 eV) of linear Dirac dispersion and interesting non-symmorphic symmetry protected surface states. The dominant features of the ZrSiS electronic structure are nodal loops which give rise to a diamond-shaped Fermi surface that is quasi-two-dimensional. Thus, the physical behavior of ZrSiS is governed by the electronic states close to the nodal loops.

We have successfully synthesized Cd_3As_2 and ZrSiS monocrystals and measured their transport and magnetic properties. Here we present a detailed study of the transport and magnetic properties of these Dirac semimetal monocrystals with controlled (reduced) charge concentration. The de Haas-van Alphen (dHvA) and the Shubnikov-de Haas (SdH) oscillations are used to probe the properties of the Fermi surface in these single crystals. Pronounced oscillations at a single frequency of 15 T were observed for Cd_3As_2 crystals. We find a Berry phase shift in the SdH oscillations, which confirms the 3D Dirac nature of the energy band dispersion in Cd_3As_2. We have also measured the magnetic torque of Cd_3As_2 and ZrSiS monocrystals by the resistive piezolever technique in the fields up to 35 T, for different temperatures and field directions. For fields along the symmetry axis, the magnetic torque of Cd_3As_2 crystals changes sign in the quantum limit. This signals a reversal of the magnetic anisotropy whereas applying a magnetic field perpendicular to the high symmetry axis, does not give this effect. This difference can be directly attributed to the topological nature of the Dirac electrons. The measured torque signal of a ZrSiS crystal consists of B^2 dependent background with quantum oscillation contributions superposed. Fourier analysis of the quantum oscillatory contribution reveals many different QO frequencies, 240 T from the petal and 600 T from the dog-bone orbits plus some clustered around 8 and 10 kT that arise from magnetic breakdown. We have found that the magnitude of the high frequency contribution is strongly dependent on the direction of magnetic field and disappears quickly by tilting away from the c-axis direction.

Poster-Mo09

Topological phase of the strained HgTe from the entanglement Hamiltonians and the first-principles calculations

Hiromu Araki,[1] Takahiro Fukui,[2] and Yasuhiro Hatsugai[3]

[1] *Graduate School of Pure and Applied Sciences, University of Tsukuba, Japan*

[2] *Department of Physics, Ibaraki University, Japan*

[3] *Division of Physics, University of Tsukuba, Japan*

For the decade, novel quantum states have been identified by topological characterization. Some of the materials are predicted as topologically non-trivial by using the first-principles calculations. Many methods to determine the topological phases of materials are developed for the identification of the materials. We are proposing a method using the entanglement Hamiltonians[1-3]. In this study, we determine the topological phases of realistic materials by using the topology of the entanglement Hamiltonians using the density functional theory (DFT) calculations.

For the typical model of the topological insulators in 2D (Kane-Mele model), we have confirmed that the Chern number of the entanglement Hamiltonian (entanglement Chern number, ECN) is consistent with the Z_2 indices for two-dimensional quantum spin Hall (QSH) phase, as $(\nu_\uparrow, \nu_\downarrow) = (1, -1)$, where the ν_σ is the ECN for the σ-spin sector [1-2]. In three dimensions, the section Chern number is defined for the two-dimensional periodic sector of the first Brillouin zone by fixing one of the wave vectors. As an analogue of the ECN for the QSH state in two-dimensions, the section ECN for the time reversal invariant (TRI) plane correspond with the weak Z_2 indices of the three-dimensional topological insulators [3]. The parity of the number of degeneracy points (Weyl points) of an entanglement Hamiltonian between the TRI planes distinguishes the strong topological insulator (STI) phase from the weak one (WTI phase) [3]. If it is odd, the phase is in the STI phase and otherwise it is WTI if the section Chern number is Z_2 non trivial.

In this study, we combine the ECN method and the DFT calculations to determine the topological phase of materials. We first compute the ground state of materials based on the DFT calculations. Next we construct a tight-binding model. Then we calculate the entanglement Hamiltonian and the entanglement (section) Chern number by the tight-binding Hamiltonian.

We have applied the method to characterize the topological phases of Bi and Sb. These materials are semimetal but we reproduced the topological phases to be (0;000) and (1;111) below the band gap [4], respectively. Also, this method is applicable to materials without inversion symmetry. We apply the method to reproduce the of the strained HgTe, which is topologically non trivial 1;(000) with strain [5].

[1] T. Fukui and Y. Hatsugai, J. Phys. Soc. Jpn., **83**, 113705 (2014)

[2] H. Araki, T. Kariyado, T. Fukui and Y. Hatsugai, J. Phys. Soc. Jpn., **85**, 043706 (2016)

[3] H. Araki, T. Fukui, and Y. Hatsugai, Phys. Rev. B, **96**, 165139 (2017)

[4] H. Araki, T. Fukui, and Y. Hatsugai, in preparation.

[5] A. A. Sultanas and D. Vanderbilt, Phys. Rev.B, **83**, 235401 (2011)

Poster-Mo10

Rashba Effect in PbSnSe Topological Crystalline Insulator Quantum Wells

M. Galicka[1], R. Rechciński[1], V.V. Volobuev[2,3], O. Caha[4], M. Simma[2], P.S. Mandal[5], E. Golias[5], J. Sánchez-Barriga[5], A. Varykhalov[5], O. Rader[5], G. Bauer[2], P. Kacman[1], G. Springholz[2], and R. Buczko*[1]

[1] *Institute of Physics, Polish Academy of Sciences, Warsaw, Poland*

[2] *International Research Centre MagTop, PL-02668 Warsaw, Poland*

[3] *Institute for Semiconductor Physics, Johannes Kepler University, Linz, Austria*

[4] *Masaryk University, Kotlářská 2, 61137 Brno, Czech Republic*

[5] *Helmholtz-Zentrum Berlin für Materialien und Energie, 12489 Berlin, Germany*

Topological crystalline insulator $Pb_{1-x}Sn_xSe$ surface quantum wells (QWs) on $Pb_{1-y}Eu_ySe$ barriers are studied experimentally and theoretically as a function of QW thickness in both the topological and trivial phases. Heterostructures with different Sn contents x were grown by molecular beam epitaxy on (111) substrates. Angle resolved photoemission (ARPES) investigations at various temperatures were carried out at the BESSY II synchrotron in Berlin. The ARPES data show well resolved size quantization of up to 10 confined electronic states with 2D energy-momentum dispersion and line width down to 10 meV. Tight-binding calculations of the dependence of the energy levels on the quantum well width are in excellent agreement with the experimental observations. It turns out that in such quantum wells the topological properties can not only be tuned by the Sn content and the temperature, but also by the quantum well thickness. This additional tuning is obtained by the thickness dependence of the hybridization gap, which results from the coupling of the topological surface and interface states.

Experiments on in-situ sub-monolayer Sn deposition on the $Pb_{1-x}Sn_xSe$ surface of the quantum well in the ARPES set-up, reveal that a strong surface Rashba effect appears in the conduction band. This is modeled using the tight-binding approach and the recursive Green's function method to derive the surface spectral density of states of the material. In our calculations we take into account that Sn covers partially, to different degrees, the surface of the quantum wells. The strong Rashba effect observed in the conduction band was simulated by applying a potential described by Thomas-Fermi screening model, similarly as it was used by us for PbSnTe films doped with Bi atoms [1]. However, since the $Pb_{1-x}Sn_xSe$ surface QWs are confined by asymmetric barriers we find that even without screening potential, a Rashba splitting can be obtained in both valence and conduction bands, due to the lack of inversion symmetry.

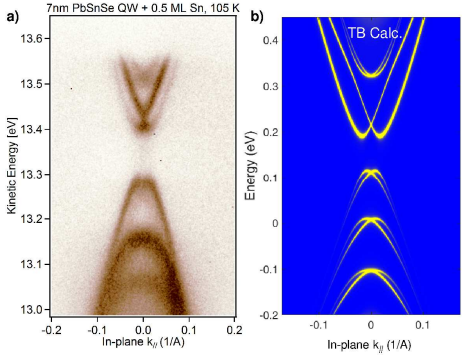

Fig.1 a) ARPES map of 7nm thick $Pb_{0.75}Sn_{0.25}Se$ QW on $Pb_{0.9}Eu_{0.1}Se$ barrier after deposition of 0.5 ML of Sn measured with a photon energy of 18 eV around the Γ point of the surface Brillouin zone; b) tight-binding spectral density of states calculated for a surface potential $V(z)=V_0e^{-z/\lambda}$ with V_0=-1.2 eV and λ=1.5nm.

[1] V. Volobuev et al., Adv. Mater. 29, 1604185 (2017).

Magneto-optical Transitions of of organic-inorganic perovskite crystals

Yongmin Kim[1], M. S. Jeong[2], H. Nojiri[3]

[1]*Department of Physics, Dankook University, Cheonan 31119, Korea*

[2]*Department of Energy Science, Sung Kyun Kwan University, Suwon 31119, Korea*

[3]*IMR, Tohoku University, Tohoku 980-8577, Japan*

Despite the vast investigations of applications on solar cell devices, there are numerous unknown basic properties of methyl-ammonium (MA) lead halides perovskite materials. In this regard, we investigate optical transitions of such crystals in high magnetic fields to 50 T. We fabricate $MAPbBr_3$ crystals by using conventional solution methods. For the photoluminescence measurements under magnetic fields, we use a 19 T cryocooled superconducting magnet and 50 T pulsed magnet. Samples show strong temperature dependency while cooling from room temperature to the liquid helium temperature. The sample show doublet transitions. High energy peak shows conventional diamagnetic shift whereas the other on the lower energy side exhibits negative shift with increasing magnetic fields. We will discuss magnetic field dependency of the optical transitions including the reduced mass and exciton diamagnetic shifts.

Poster-Mo12

Shubnikov-de Haas oscillations in back-gated few-layer WSe_2 Hall bars

Banan Kerdi,[1] Mathieu Pierre,[1] Michel Goiran,[1] and Walter Escoffier[1]

[1] *Laboratoire National des Champs Magnétiques Intenses (LNCMI), Université de Toulouse, INSA, UPS, UGA, CNRS UPR 3228, EMFL, Toulouse, France*

We fabricated WSe_2 devices in order to perform electronic transport measurements under high magnetic field. Few-layer flakes of WSe_2 were deposited on h-BN flakes, etched in a Hall bar configuration, and electrically contacted with Pt/Au electrodes. We performed transport measurements under pulsed magnetic field up to 55 T and at low temperature (4.2 K). By applying a negative gate voltage to the substrate, we were able to investigate the hole conduction regime, despite non-ohmic contacts. While very little magnetoresistance is observed, clear $1/B$-periodic conductance oscillations appear above 20 T. A single frequency is observed for low carrier density and additional features rise at large negative gate voltage. The transverse Hall voltage was simultaneously measured. We extract information on the carrier concentration, their mobility and effective mass, as well as their degeneracy. Our fabrication process allows to obtain devices with sufficient mobility to reach the quantum transport regime. Work is under progress to improve the device mobility and the ohmicity of the contacts.

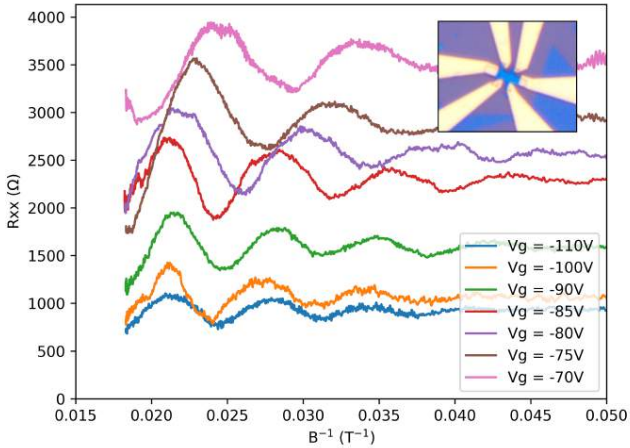

FIG. 1. *Longitudinal resistance of a WSe_2 Hall bar device, measured at 4.2 K and up to 55 T for several back-gate voltages. A small background has been substracted. Shubnikov-de Haas oscillations are oberved, with a gate-dependant period, ranging from 150 T at $V_g = -110$ V to 105 T at $V_g = -70$ V. Insert: optical microscope image of the 1.5 µm-wide WSe_2 Hall bar.*

Poster-Mo13

Spin Hall Effect in Antiferromagnets

Sverre A Gulbrandsen,[1] Camilla Espedal,[1] and Arne Brataas[1]

[1] *Center for Quantum Spintronics, Department of Physics, Norwegian University of Science and Technology, NO-7491 Trondheim, Norway*

Recent experiments demonstrate that antiferromagnets exhibit a spin Hall effect. Calculations also indicate that the intrinsic contribution is important in determining the magnitude of the spin Hall angle. However, we do not know how the mean free path, exchange interaction, and spin-orbit coupling govern these results and how these factors might influence our understanding of experiments. To address these questions, we consider a minimal model of an antiferromagnet. We numerically compute the spin Hall conductance as a function of impurity concentration, exchange energy, and spin-orbit coupling. We find that the spin Hall conductance is considerably larger in antiferromagnetic systems compared to normal metals. This opens yet another avenue of using antiferromagnets in spintronics devices.

Poster-Mo14

Variable range hopping conduction and magnetoresistance in ordered defect compounds.

L. Essaleh [1], S. M. Wasim [2], G. Marín [3], C. Rincón [2], S. Amhil [1], J. Galibert [4]

[1] *Laboratory of Condensed Matter and Nanostructures (LMCN), Cadi-Ayyad University, Faculty of Sciences and Technology, Department of Applied Physics, Marrakech, Morocco.*

[2] *Centro de Estudios de Semiconductores, Facultad de Ciencias. Universidad de Los Andes, Mérida 5101, Venezuela.*

[3] *Laboratorio de Estructura e Ingeniería de Materiales Nanoestructurados (LEIMN), Centro de Investigación y Tecnología de Materiales (CITeMa), InstitutoVenezolano de InvestigacionesCientíficas (IVIC), Maracaibo 4011, Venezuela.*

[4] *Laboratoire National des Champs Magnétiques Intenses, LNCMI-EMFL, CNRS/INSA/UGA/UPS, Toulouse & Grenoble, France.*

Among the Cu-ternaries compounds of the Cu-III-VI_2 family used for photovoltaic conversion (like $CuInSe_2$), the compounds of the Cu-III_3-VI_5 family are expected also to play an important role in energy conversion devices. Because these compounds have a deficiency of one cation over the anions they were originally referred to as Ordered Vacancy Compounds (OVC). We report here on the electrical resistivity in a wide temperature range to establish the type of conduction mechanism and also the variation of magnetoresistance (MR) up to 30 T at different temperatures for some representative OVC compounds. The results are analysed and compared with the existing theoretical models.

In p type $CuGa_3Te_5$ **[1]** variable range hopping conduction (VRH) of Efros-Shklovskii type (ES) for a vanishing density of states, when a Coulomb gap due to repulsive interaction of free carriers appears at the Fermi level, is observed in the temperature range [4-150 K]. This type of electrical conduction over such a wide temperature range is possibly due to very low concentration of charge carriers as compared to the critical concentration Nc that define the Mott's metal-insulator transition (MIT). The MR is positive in all over the magnetic field range and between 4 and 40 K. Its behaviour both at low and high field up to 30 T is analysed in the framework of the ES theoretical model for VRH. To our knowledge this study is the only work where the proposed model for the variation of MR when the conduction is of a ES-VRH type, is confirmed. This has not been reported in either I-III-VI_2 or any I-III_3-VI_5 compounds.

In n-$CuIn_3Se_5$ **[2]** VRH of Mott type is observed for the first time in such a kind of OVC in two different temperature range between 10K and 65K. As for the case of CuGa3Te5, the MR is positive. The analysis of the magnetic field dependence of the MR confirms a ES-VRH behaviour.

In p-$CuIn_3Te_5$ **[3]** an other type of OVC, Mott type of VRH conduction is observed in wide temperature range [45-210 K]. The low magnetic field negative magnetoresistance (NMR) is observed, and is explained to be due to the quantum interferences between many path connecting impurity sites during the hopping process *(model of N'Guyen, Spivak & Shklovskii-NSS-)*. The magnetic field dependence of the MR at different temperatures, is explained with the theoretical model for Mott-type VRH. To our knowledge, this study is the only work where the proposed model for the variation of MR when VRH is of Mott type is confirmed over a wide temperature range up to 210 K in an ODC material.

[1] S.M Wasim, L. Essaleh, G. Marín, C. Rincón, S. Amhil, J. Galibert Superlattices and Microstructures 107, 285 (2017)
[2] S.M. Wasim, L. Essaleh, G. Marín, J. Galibert Materials Research Bulletin 87, 219 (2017)
[3] L. Essaleh, S.M. Wasim, G. Marín, C. Rincón, S. Amhil, J. Galibert J. Applied Physics 122, 015702 (2017)

Poster-Mo15

Large-scale impurity potential in HgTe quantum wells with inverted band structure

Ilchenko E.V.[1], Popov M.R.[1], Neverov V.N.[1], Podgornykh S.M.[1], Gudina S.V.[1], Novik E.G. [2], Shelushinina N.G.[1], Dvoretskii S.A.[3], Mikhailov N.N.[3] and Yakunin M.V.[1]

[1]*Miheev Institute of Metal Physics, Ural Branch, Russian Academy of Sciences, Yekaterinburg, Russia*

[2] *Institute for Theoretical Physics and Astrophysics, University of Würzburg, D-97074 Würzburg, Germany*

[3]*Rzhanov Institute of Semiconductor Physics, Siberian Branch, Russian Academy of Sciences, Novosibirsk, Russia*

The longitudinal and Hall resistances were measured in HgTe / HgCdTe structures with a quantum well width of 20.3 nm at T = (2.9-50) K in magnetic fields up to 9 T. Conductivity analysis in the quantum Hall effect regime (QHE) made it possible to conclude that the large-scale random potential plays a decisive role in the conductivity processes in the structures under study.

In the plateau-plateau transition region the real scaling behavior [1, 2] is observed in a wide temperature interval T = (2.9-30) K, the value of critical exponent is in good agreement with the experimental data for systems with large-scale impurity potential [3].

The study of thermoactivation conductivity $\sigma_{xx} = \sigma_0 \exp(-E_A / T)$ in the areas of the QHE plateau made it possible to determine the values of the energy gaps between the Landau levels which is in a good agreement with the results of calculations of the band structure in the framework of the **kp** model. The value of thermoactivation conductivity prefactor $\sigma_0 \cong 2\,e^2/h$ indicates the large-scale nature of the impurity potential [4].

It was found that the density of localized states (DOS) in the in the mobility gaps (in the middle of the gap where the filling factor is close to an integer value) is comparable to the DOS value for a 2D electron gas without a magnetic field, which can be explained in the framework of the concepts of nonlinear screening in a long-range random potential in combination with the oscillating dependence of DOS on the filling factor [5 and references therein].

Temperature-induced conductivity in QHE plateau region was described in terms of variable range hopping conductivity [6]. The localization length critical exponent value corresponding to result of the classical percolation theory for long-range impurity potential was received. It was shown that such a regime of hopping conductivity observing far from the Landau level center is agreed with hops on localized states in the tails of broadened Landau levels out of quantum tunneling regime, i.e. in the classical percolation theory region.

It is shown that the dependence of the minimum values of the localization length correlates with the dependence of the cyclotron radius but not the magnetic length in accordance with the predictions of [7]. The fact that localization length is 10 times more than cyclotron radius evidences to the long-range character of the random impurity potential.

[1] B. Huckestein, Rev.Mod.Phys. **67**, 357 (1995).
[2] A.M.M. Pruisken, Phys.Rev.Lett. **61**, 1297 (1988).
[3] W. Li et al., Phys.Rev.Lett. 94, 206807 (2005); Phys.Rev.Lett. **102**, 216801 (2009).
[4] D.G. Polyakov, B.I. Shklovskii, Phys.Rev.Lett. **74**, 150 (1995).
[5] A.L. Efros, F.G. Pikus, V G. Burnett, Phys.Rev.B **47**, 2233 (1993).
[6] D.G. Polyakov, B.I. Shklovskii, Phys.Rev.B **48**, 11167 (1993).
[7] M.M. Fogler, A.Yu. Dobin, B.I. Shklovskii, Phys.Rev. B **57**, 4614 (1998)

Poster-Mo16

Effect of illumination on quantum lifetime in GaAs quantum wells

Xiaojun Fu,[1] Ausin Riedl,[1] Mikhail Borisov,[1] Michael Zudov,[1] John Watson,[2,3] Geoffrey Gardner,[3,4] Michael Manfra,[2,3,4,5] Kirk Baldwin,[6] Loren Pfeiffer,[6] and Kenneth West[6]

[1] *School of Physics and Astronomy, University of Minnesota, Minneapolis, Minnesota 55455, USA*

[2] *Department of Physics and Astronomy, Purdue University, West Lafayette, Indiana 47907, USA*

[3] *Birck Nanotechnology Center, Purdue University, West Lafayette, Indiana 47907, USA*

[4] *School of Materials Engineering, Purdue University, West Lafayette, Indiana 47907, USA*

[5] *Station Q Purdue and School of Electrical and Computer Engineering, Purdue University, West Lafayette, Indiana 47907, USA*

[6] *Department of Electrical Engineering, Princeton University, Princeton, New Jersey 08544, USA*

It is known that low-temperature illumination of a two-dimensional electron gas (2DEG) in GaAs/AlGaAs quantum wells can improve the quality of magnetotransport data even when the carrier density and mobility remain essentially unchanged. In high magnetic fields, this improvement is manifested by a better development of fragile fractional and re-entrant integer quantum Hall states in the $N = 1$ Landau level and occurs in structures employing both conventional δ-doping directly in the AlGaAs barrier [1] and in modern devices utilizing "doping well" design [2]. While the exact cause for this improvement remains unclear, it has been speculated that it might stem from an increased number of neutral shallow donors [1] or redistribution of charge in the donor layer [2] leading to enhanced screening of remote impurities (RI) and/or better homogeneity of the 2DEG.

In this work we (i) examine the effect of illumination on the quality of the low-field magnetotransport and (ii) quantitatively assess improved screening by investigating the effect of illumination on total (quantum) electron-impurity scattering time τ_q which is expected to be sensitive by RI scattering. To measure τ_q we employ microwave-induced resistance oscillations (MIRO) [3] which, in contrast to Shubnikov-de Haas oscillations, are believed to be largely immune to macroscopic density fluctuations and do not require very slow magnetic field sweeps. Since the MIRO amplitude is proportional to $\lambda^2 = e^{-\epsilon/f\tau_q}$ (here, $\epsilon = 2\pi f/\omega_c$, f is the microwave frequency, and ω_c is the cyclotron frequency), τ_q is readily available from the Dingle analysis. We have investigated several samples with essentially identical outcomes. As shown in Fig. 1(a), MIRO quality improves dramatically after illumination; oscillations become more pronounced and extend to much lower magnetic fields (higher ϵ). At the same time, the density and the mobility remain essentially unchanged. The Dingle plot analysis, illustrated in Fig. 1(b), reveals that the observed improvement is a result of significant enhancement of τ_q which increases by a factor of about two, from ≈ 23 ps to ≈ 44 ps. We believe that this increase presents strong evidence that illumination results in better screening of the random potential from ionized impurities, presumably due to light-assisted redistribution of charge in the doping layers. However, whether the observed increase in τ_q is directly correlated with high-field transport characteristics remains an open question.

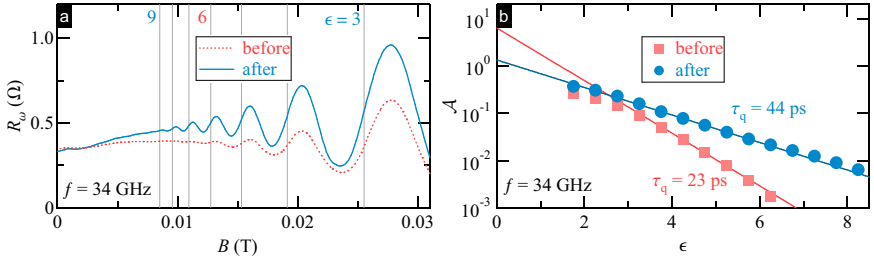

FIG. 1. *(a) Magnetoresistance $R_\omega(B)$ measured under microwave irradiation of frequency $f = 34$ GHz before (dotted line) and after (solid line) illumination. (b) Reduced MIRO amplitude $\mathcal{A}$ vs ϵ before (squares) and after (circles) illumination.*

[1] G. Gamez and K. Muraki, Phys. Rev. B **88**, 075308 (2013).
[2] M. Samani, A. V. Rossokhaty, E. Sajadi, S. Lüscher, J. A. Folk, J. D. Watson, G. C. Gardner, and M. J. Manfra, Phys. Rev. B **90**, 121405 (2014).
[3] M. A. Zudov, R. R. Du, J. A. Simmons, and J. L. Reno, Phys. Rev. B **64**, 201311(R) (2001).

Electro-optical properties of a D_2^+ molecular complex confined in an elliptical $Ga_{1-x}Al_xAs$ nanodisk

M.Contreras,[2,*] Eugenio Giraldo,[3] J.L.Palacio[1,2] M. R. Fulla,[1,2,] Guillermo L. Miranda,[3] and J. H. Marín[1]

[1] *Universidad Nacional de Colombia Sede Medellín, AA 3840 Medellín, Colombia*
[2] *Institución Universitaria Pascual Bravo, AA 6564 Medellín, Colombia*
[3] *Universidad EIA, Código Postal: 055428, Envigado, Colombia*
*Corresponding author: *marlonfulla@yahoo.com*

Very recently, the manufacturing of new low-dimensional nanostructures has rapidly evolved allowing to obtain diverse and exotic morphologies such as the Pr-doped ZnO/SnO2 nanoflowers [1], ZnO nanospindles [2], and being of special interest, the graphene nanoflakes [3]. The range of applications varies from materials reinforcement [3], gas sensors [1], field emission displays [2], among others. A detailed study of the morphology of these nanosystems have been performed by scanning/transmission electron microscopy techniques, X-ray diffraction and energy dispersive X-ray spectroscopy [2]. Their composition and optical responses have been characterized via photoluminescence techniques [3]. In particular, the experimental studies reporting nanoflakes with different shapes, sizes, compositions and irregularities, motivate the formulation of theoretical models to study the quantum confinement of few-particle systems in such nanostructures in order to tailor customizable few-particle energy spectra.

These remarkable findings, have motivated the present contribution in which is analyzed the energy structure of an artificial $D2^+$ molecular complex confined in a non-uniform elliptical $Ga1-xAlxAs$ nanodisk. The energy structure is analyzed within the effective mass framework by using an adiabatic/finite elements hybrid technique. In addition, the optical response is investigated within the compact density matrix formalism. Validation of the numerical procedure was carried out through the comparison with analytic solutions (like those obtained for single- electron disks) showing a good accordance between the set of results.

References

[1] Q. Ge, S.Y. Ma, Y.B. Xu, X.L. Xu, H. Chen, Z. Qiang, H.M. Yang, L. Ma and Q.Z. Zeng, Mater. Lett. 191 5 (2017).
[2] Fei Li, Wentuan Bi, Luoyuan Liu, Zhen Li and Xintang Huang, Colloid Surf. APhysicochem. Eng. Asp. 334 160 (2009).
[3] Zhen Cao, Xudong Wang, Jiongli L, YueWu, Haiping Zhang, Jianqiang Guo and Shengqiang Wang, J. Alloys Compd. 696, 498 (2017).

Poster-Mo18

Non-equidistant Landau levels in Germanium

Iris Crassee,[1] Artur Slobodeniuk,[1] Gerard Martinez,[1] Iwona Pasternak,[2] Wlodek Strupinski,[3] Milan Orlita,[1,4] and Marek Potemski[1]

[1] *Laboratoire National des Champs Magnétiques Intenses, CNRS-UGA-UPS-INSA, Grenoble, France*

[2] *Warsaw University of Technology, Warsaw, Poland*

[3] *Institute of Electronic Materials Technology, Warsaw, Poland*

[4] *Institute of Physics, Charles University, Praha, Czech Republic*

Germanium, a common semiconductor, played an important role in early semiconductor physics. Due to its relatively small band gap, nowadays it is mostly used for optical applications like in the solar cell industry, LEDs and fiber optics. The electronic and optical properties of germanium have been the subject of numerous studies. Several magneto-optical studies at moderate fields, reveal thermal donors that can give rise to a series of magneto-optical resonances in the infrared regime [1,2]. In addition, in hole-doped germanium, the heavy and light hole bands show a non-parabolicity giving rise to a series of Landau levels (LLs) in the terahertz regime. The LLs originating from the light band and the cyclotron resonance from the heavy band can be pumped creating a population inversion; tunable germanium lasers operate in the terahertz regime [3].

We present a magneto-optical spectroscopy study of germanium using magnetic fields up to 32 T. We show that undoped germanium, annealed at high temperature displays a rich magneto-optical response in the far and mid infrared range. Already at 0.5T LL excitations can be observed, while at around 4T as much as 17 individual LL transitions are found. Surprisingly, the LLs in the mid infrared regime show an almost perfect square-root dependence on both magnetic field and LL number. The square-root dependence of the levels found in high temperature annealed germanium is both unexpected and remarkable as these are the magneto-optical signatures of relativistic carriers generally found in novel (relativistic) materials such as graphene [4-5], topological insulators and semimetals like Cd_3As_2 [6].

[1] W. J. Moore, J. Phys. Chem. Solids 32, 93 (1970)
[2] P. Clauws *et al.*, Phys Rev B 44, 3665 (1991)
[3] I. Hosako and N. Hiromoto, J of the Communications Research Laboratory 49, 81 (2002)
[4] M. Sadowski *et al.*, Phys Rev Lett. 97, 266405 (2006)
[5] I. Crassee *et al.*, Nature Phys. 7 48 (2011)
[6] A. Akrap *et al.*, Phys Rev Lett. 117 136401 (2016)

Poster-Mo19

Electrical Characteristics of Graphene/GaN Schottky Junction

Sung-Nam Lee,[1] Hyunsoo Kim[2]

[1]*Department of Nano-Optical Engineering, Korea Polytechnic University, Siheung 15073, Republic of Korea*
[2]*School of Semiconductor and Chemical Engineering, Semiconductor Physics Research Center, Chonbuk National University, Jeonju 54896, Republic of Korea*

Two-dimensional hexagonal carbon array, also known as graphene, has been extensively studied for application as an active or passive layer in electronic and optoelectronic semiconductor devices due to its outstanding physical and optical characteristics, including high intrinsic electron mobility, quantum electronic transport, low optical absorption, and good chemical and mechanical stability [1,2]. In particular, good electrical conductivity and excellent optical transparency across the entire spectrum of wavelengths of graphene made it a promising candidate for use as a transparent contact in optoelectronic devices such as solar cells and light-emitting diodes (LEDs).

Recently, a number of studies focusing on the application of graphene transparent p-contacts in GaN-based light-emitting diodes have been reported by several groups [3,4]. In addition, an electrically rectifying behavior was also observed for the graphene contact formed on n-type GaN [5], suggesting that the graphene on n-GaN be a promising candidate for the Schottky rectifiers. However, this finding is strange considering that the Schottky barrier height expected to form at graphene/n-GaN interface is as low as ~0.4 eV due to the small work-function difference between graphene and n-GaN, implying that the graphene contact to n-GaN should produce poor rectifying behavior. Furthermore, the experimentally obtained Schottky barrier height of 0.74 eV [5] was even larger than the predicted value. These inconsistent results indicate that, for the successful development of graphene integrated GaN-based semiconductor devices, the electrical characteristics and carrier transport mechanism of graphene-GaN contact should be thoroughly investigated [6]. However, in-depth comprehensive studies on this subject are still lacking.

In this study, the electrical characteristics of graphene Schottky contacts formed on undoped GaN semiconductor were investigated. Excellent rectifying behavior with a rectification ratio of ~10^7 at ±2 V and a low reverse leakage current of 1.0×10^{-8} A/cm^2 at −5 V were observed. The Schottky barrier height, as determined by the thermionic emission model, Richardson plots, and barrier inhomogeneity model, were 0.90, 0.72, and 1.24±0.13 eV, respectively. Despite the predicted low barrier height of ~0.4 eV at graphene-GaN interface, the formation of excellent rectifying characteristics with much larger barrier height is attributed to the presence of a large number of surface states (1.2×10^{13} states/cm^2/eV) and the internal spontaneous polarization field of GaN, resulted in a significant upward surface band bending or a bare surface barrier height as high as of 2.9 eV. Using the *S* parameter of 0.48 (measured from the work function dependence of Schottky barrier height) and the mean barrier height of 1.24 eV, the work function of graphene in Au/graphene/GaN stack could be approximately estimated to be as low as 3.5 eV. The obtained results indicate that graphene is a promising candidate for use as a Schottky rectifier in the GaN semiconductors with n-type conductivity.

[1] Novoselov et al. Science, 306, 666, (2004)
[2] Geim et al. Nat. Mater, 6, 183, (2007)
[3] Jo et al. Nanotechnology, 21, 175201, (2010)
[4] Chandramohan et al. ACS Appl. Mater. Interfaces, 5, 958, (2013)
[5] Tongay et al. Phys. Rev. X, 2, 011002, (2012)
[6] Kim et al. Nano Res. 8, 1327, (2015)

Address correspondence to Hyunsoo Kim, hskim7@jbnu.ac.kr

Poster-Mo20

Non equilibrium anisotropic excitons in atomically thin ReS_2

J. M. Urban,[1] M. Baranowski,[1,2] A. Kuc,[3] Ł. Kłopotowski,[4] A. Surrente,[1] Y. Ma,[3] D. Włodarczyk,[4] A. Suchocki,[4] D. Ovchinnikov,[5] T. Heine,[3] D. K. Maude,[1] A. Kis,[5] and P. Plochocka[1]

[1] *Laboratoire National des Champs Magnétiques Intenses, UPR 3228, CNRS-UGA-UPS-INSA, Grenoble and Toulouse, France*

[2] *Department of Experimental Physics, Faculty of Fundamental Problems of Technology, Wroclaw University of Science and Technology, Wroclaw, Poland*

[3] *Wilhelm-Ostwald Institute für Physikalische und Theoretische Chemie, Universität Leipzig, Linné Str. 2, 04103 Leipzig, Germany*

[4] *Institute of Physics, Polish Academy of Sciences, Al. Lotników 32/46, 02-668 Warsaw, Poland*

[5] *Electrical Engineering Institute and Institute of Materials Science and Engineering, École Polytechnique Fédérale de Lausanne, CH-1015 Lausanne, Switzerland*

Rhenium disulfide is a member of the family of rapidly emerging transition metal dichalcogenides. It has gained particular interest due to its environmental stability and pronounced in-plane anisotropy of the optical and electrical properties, stemming from the low symmetry of its distorted 1T' lattice [1,2].

Despite intensive investigation the character of the ReS_2 badgap still raises controversy. Here we show detailed investigations of the optical properties of ReS_2 flakes with a different number of layers which allowed us to conclude on the indirect character of the fundamental bandgap from bulk to monolayer. We observed linearly polarized photoluminescence from two non-degenerate excitonic states X_1 and X_2. The weak PL intensity as well as the simultaneous observation of X_1 and X_2 emission suggest hot-carrier nature of the photoluminescence and the presence of a lower indirect bandgap which provides a non radiative relaxation pathway. We discuss the experimental results in the light of DFT calculations and predictions of a model based on rate equations [3].

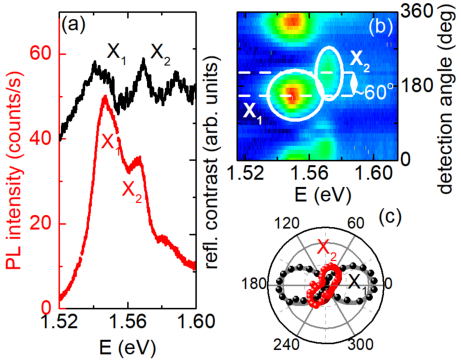

FIG. 1. *(a) PL spectra of bulk-like part of the sample measured at 10K (red curve) together with the reflection contrast spectra (black curve). (b) PL spectra as a function of the linear polarization detection angle. (c) Polar plot of the PL intensity of X_1 (blue balls) and X_2 (red balls) excitons as a function of polarization detection angle together with the fitted curves. For clarity points on polar plot are shifted by about 25° comparing to results presented in panel (b).*

[1] O. B. Aslan, *et al.*, ACS Photonics **3**, 96 (2016)

[2] A. Arora, *et al.*, Nano Letters **17**, 3202 (2017)

[3] J. M. Urban, M. Baranowski *et al.*, *submitted*

Study of magneto-plasmon resonances in the photo-excited GaAs/AlGaAs 2D electron system

A. Kriisa,[1] R. Samaraweera,[1] M. Heimbeck,[2] H. O. Everitt,[2,3] C. Reichl,[4] W. Wegscheider,[4] R. G. Mani[1]

[1]*Dept. of Physics & Astronomy, Georgia State University, Atlanta, GA 30303*

[2]*Army Aviation & Missile RD&E Center, Redstone Arsenal, Huntsville, AL 35898*

[3]*Depts. of Physics and ECE, Duke University, Durham, NC 27708*

[4]*Laboratorium für Festkörperphysik, ETH-Zürich, 8093 Zürich, Switzerland*

Microwave-induced zero-resistance-states in the photo-excited high quality GaAs/AlGaAs system evolve from the minima of microwave photo-excited 1/4-cycle shifted magnetoresistance oscillations.[1] Such magnetoresistance oscillations are thought to exhibit nodes at cyclotron resonance, and cyclotron resonance harmonics. The effective mass extracted from the radiation-induced magnetoresistance oscillations is known to differ from the standard effective mass ratio for electrons in the GaAs/AlGaAs system.[1] To identify the origin of this difference, we have looked for the effective mass in the magnetoplasmon resonance (MPR) in the microwave/terahertz reflection from the high mobility 2DES and attempted to correlate the observations with observed oscillatory magnetoresistance over the $30 < f < 330$ GHz band. For linearly polarized microwave/terahertz photo-excitation over the examined frequency band, experiments indicate strong reflection resonance on both sides of the magnetic field axis, see Fig. 1. In addition, there is evidence for electronic heating in the vicinity of MPR, which is indicated by a reduced amplitude of the Shubnikov-de Haas oscillations. Such results are correlated here to extract the plasmon frequency, the cyclotron effective mass, and the single particle lifetime at low magnetic fields and high filling factors in the confined GaAs/AlGaAs 2D system. Further, the extracted effective mass is then compared with the effective mass determined from the radiation-induced magnetoresistance oscillations.

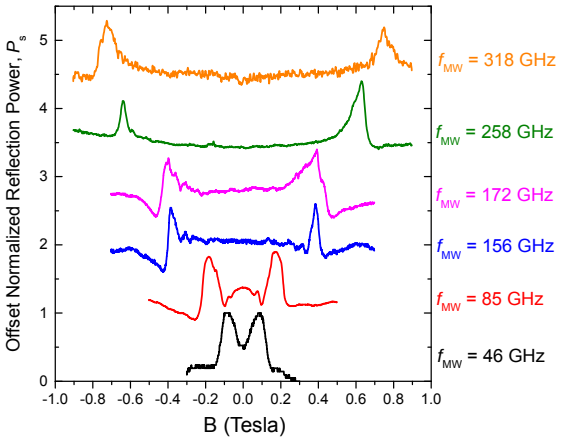

Fig. 1. The reflection signal from the microwave and terahertz photo-excited GaAs/AlGaAs 2D electron system. Magnetoplasmon resonances are observable for both directions of the magnetic field for linearly polarized photoexcitation. The results serve to determine the effective mass and the plasmon frequency in this confined 2D system.

[1] R. G. Mani, J. H. Smet, K. von Klitzing, V. Narayanamurti, W. B. Johnson, V. Umansky, Phys. Rev. Lett. 92, 146801(2004)

Poster-Mo22

Variable range hopping conduction and magnetoresistance in ordered defect compounds.

L. Essaleh [1], S. M. Wasim [2], G. Marín [3], C. Rincón [2], S. Amhil [1], J. Galibert [4]

[1] *Laboratory of Condensed Matter and Nanostructures (LMCN), Cadi-Ayyad University, Faculty of Sciences and Technology, Department of Applied Physics, Marrakech, Morocco.*

[2] *Centro de Estudios de Semiconductores, Facultad de Ciencias. Universidad de Los Andes, Mérida 5101, Venezuela.*

[3] *Laboratorio de Estructura e Ingeniería de Materiales Nanoestructurados (LEIMN), Centro de Investigación y Tecnología de Materiales (CITeMa), InstitutoVenezolano de InvestigacionesCientíficas (IVIC), Maracaibo 4011, Venezuela.*

[4] *Laboratoire National des Champs Magnétiques Intenses, LNCMI-EMFL, CNRS/INSA/UGA/UPS, Toulouse & Grenoble, France.*

Among the Cu-ternaries compounds of the Cu-III-VI_2 family used for photovoltaic conversion (like $CuInSe_2$), the compounds of the Cu-III_3-VI_5 family are expected also to play an important role in energy conversion devices. Because these compounds have a deficiency of one cation over the anions they were originally referred to as Ordered Vacancy Compounds (OVC). We report here on the electrical resistivity in a wide temperature range to establish the type of conduction mechanism and also the variation of magnetoresistance (MR) up to 30 T at different temperatures for some representative OVC compounds. The results are analysed and compared with the existing theoretical models.

In p type $CuGa_3Te_5$ **[1]** variable range hopping conduction (VRH) of Efros-Shklovskii type (ES) for a vanishing density of states, when a Coulomb gap due to repulsive interaction of free carriers appears at the Fermi level, is observed in the temperature range [4-150 K]. This type of electrical conduction over such a wide temperature range is possibly due to very low concentration of charge carriers as compared to the critical concentration Nc that define the Mott's metal-insulator transition (MIT). The MR is positive in all over the magnetic field range and between 4 and 40 K. Its behaviour both at low and high field up to 30 T is analysed in the framework of the ES theoretical model for VRH. To our knowledge this study is the only work where the proposed model for the variation of MR when the conduction is of a ES-VRH type, is confirmed. This has not been reported in either I-III-VI_2 or any I-III_3-VI_5 compounds.

In n-$CuIn_3Se_5$ **[2]** VRH of Mott type is observed for the first time in such a kind of OVC in two different temperature range between 10K and 65K. As for the case of CuGa3Te5, the MR is positive. The analysis of the magnetic field dependence of the MR confirms a ES-VRH behaviour.

In p-$CuIn_3Te_5$ **[3]** an other type of OVC, Mott type of VRH conduction is observed in wide temperature range [45-210 K]. The low magnetic field negative magnetoresistance (NMR) is observed, and is explained to be due to the quantum interferences between many path connecting impurity sites during the hopping process *(model of N'Guyen, Spivak & Shklovskii-NSS-)*. The magnetic field dependence of the MR at different temperatures, is explained with the theoretical model for Mott-type VRH. To our knowledge, this study is the only work where the proposed model for the variation of MR when VRH is of Mott type is confirmed over a wide temperature range up to 210 K in an ODC material.

[1] S.M Wasim, L. Essaleh, G. Marín, C. Rincón, S. Amhil, J. Galibert Superlattices and Microstructures 107, 285 (2017)
[2] S.M. Wasim, L. Essaleh, G. Marín, J. Galibert Materials Research Bulletin 87, 219 (2017)
[3] L. Essaleh, S.M. Wasim, G. Marín, C. Rincón, S. Amhil, J. Galibert J. Applied Physics 122, 015702 (2017)

Poster-Mo23

Homotopy oddness manifestation in unconventional FQHE observed in bilayer graphene

Janusz E. Jacak[1]

[1] *Department of Quantum Technologies, Wroclaw University of Science and Technology, Wroclaw, Poland*

Recent experimental observations of FQHE in bilayer graphene in first eight subbands of Landau levels in open-face hBN embedded samples [1] and in the lowest LL in suspended sample [2] reveal an unconventional hierarchy of FQHE different than the Hall hierarchy in graphene monolayer and in conventional 2DEG in GaAs. We explain this behavior within the topological approach to strongly correlated incompressible Hall states and achieve a consistence of the model with the available experimental data. We identify the oddness of FQHE hierarchy in graphene bilayer with not exact 2D topology when carriers can tunnel between two sheaths of the sample. This property changes the homotopy classes of braids resulting in observed differences of FQHE hierarchy in bilayer graphene in comparison to monolayer one. We have proposed an experimental confirmation of this topological effect by application of a vertical voltage perpendicular to a basal surface which would block tunneling of electrons in one direction. As for hopping of braids between two sheaths the tunneling of electrons is necessary in both opposite directions, the applied vertical field may change the homotopy-class of bilayer sample and restore the braid homotopy to that one of a monolayer system. We report the experimental verification of this effect [3].

[1] Diankov G, Liang C T, Amet F, Gallagher P, Lee M, Bestwick A J, Tharratt K, Coniglio W, Jaroszynski J, Watanabe K, Taniguchi T and Goldhaber-Gordon D, Nature Comm., **7**, 1390, (2016)

[2] Ki D, Falko V, Abanin D and Morpurgo A, Nano Lett., **14**, 2135, (2014)

[3] Maher P, Wang L, Gao Y, Forsythe C, Taniguchi T, Watanabe K, Abanin D, Papic Z, Cadden-Zimansky P, Hone J, Kim P and Dean C R, Science, **345**, 61, (2014)

Poster-Mo24

Two component superfluid Bose-Einstein condensate of indirect excitons in twin Hall systems complementary filled

Janusz E. Jacak[1]

[1] *Department of Quantum Technologies, Wroclaw University of Science and Technology, Wroclaw, Poland*

We develop the model of interlayer coupling of electrons and holes in Landau levels complementary filled, $\nu_{top}+\nu_{bot}=1$, in twin parallel Hall systems separated by an insulating barrier. Taking into account the opposite vertical polarizations of resulting interlayer excitons we propose a two fluid model for related Bose-Einstein condensate of excitons. This model allows for optimization of repulsion of excitons in condensates resulting in their superfluidity. This repulsion needs a specific striping in k-space of carrier local density leading to an energy competition with the reentrant IQHE in striped structure in the twin-layer Hall system. By application of the quantum Monte-Carlo simulation we have identified the phase diagram of the superfluid and IQH phases in the twin Hall system with respect to its filling scheme and the barrier thickness in both experimental configurations, counterflow or drag ones. We have achieved a consistence of the model with experimentally observed superfluid-IQHE phenomena in two measured systems: twin parallel Hall GaAs system separated by GaAlAs barrier and twin bilayer-graphne Hall system separated by hBN barrier. We have explained the puzzled observations of disappearance of the Hall response in drag configuration at $(-1/2,-1/2)$ scheme of filling, the absence of the counterflow response of $n=1$ LLL states in bilayer-graphene, as well as we have achieved the quantitative consistence of the model phase diagram details with the experimental data (including energy activation values and the shape and positions of the transition curves).

Quantum Hall states in an anisotropic bulk Weyl semimetal TaAs

Jianfeng Zhang[1], Xiaohu Zheng[1], Haiwen Liu[2], Jian Mi[1], Zhujun Yuan[1],Chenglong Zhang[1], Shuang Jia[1], Xincheng Xie[1], Rui-Rui Du[1], Chi Zhang[1]

1. International Center for Quantum Materials, Peking University, Beijing, China.
2. Department of Physics, Beijing Normal University, Beijing, China.

Our study reports the two-dimensional (2D)-like Shubnikov-de Hass (SdH) oscillations accompanied by quantized Hall resistivity in the high mobility (multi-quantum layers) TaAs crystal with c- (001) sample surface. On the other hand, there is no quantum Hall (QH) plateau with the single crystal sample of a-(100) crystalline surface. Moreover, microwave photovoltage (PV) and photocurrent (I_{ph}) present distinct 2D-like quantum oscillations and QH states with beautifully features. PV and I_{ph} minima appear at more Landau level fillings, because the QH degeneracy is broken further. Microwave enhances the conductivity and mobility within the skin depth of the electromagnetic field, thus more QH features are observed. Thus our work shows important implications for transport studies of 3D topological materials.

Poster-Mo26

Dephasing in Mach-Zehnder interferometer by an Ohmic contact

Edvin G. Idrisov,[1,2] Ivan P. Levkivskyi,[3,4,5] and Eugene V. Sukhorukov[2]

[1] *Physics and Materials Science Research Unit, University of Luxembourg, 1511 Luxembourg, Luxembourg*
[2] *Département de Physique Théorique, Université de Genève, CH-1211 Genève 4, Switzerland*
[3] *Theoretische Physik, ETH Zurich, CH-8093 Zurich, Switzerland*
[4] *Institute of Ecology and Evolution, University of Bern, CH-3012 Bern, Switzerland*
[5] *Department of Computational Biology, University of Lausanne, CH-1011 Lausanne, Switzerland*

We study dephasing in an electronic Mach-Zehnder (MZ) interferometer based on quantum Hall (QH) edge states by a micrometer-sized Ohmic contact embedded in one of its arms. We find that at the filling factor $\nu = 1$, as well as in the case where an Ohmic contact is connected to an MZ interferometer by a quantum point contact (QPC) that transmits only one electron channel, the phase coherence may not be fully suppressed. Namely, if the voltage bias $\Delta\mu$ and the temperature T are small compared to the charging energy of the Ohmic contact E_C, the free fermion picture is manifested, and the visibility saturates at its maximum value. At large biases, $\Delta\mu \gg E_C$, the visibility decays in a power-law manner. At high temperatures, $T \gg E_C$, the visibility decays exponentially with temperature.

[1] Edvin G. Idrisov *et al.*, arXiv:1712.00824, (December) 2017

Poster-Mo27

Scaffold-free and label-free biofabrication technology using levitational assembly in high magnetic field

Vladislav Parfenov[1], Elizaveta Koudan[1], Pavel Karalkin[1], Frederico Pereira[1] Elena Bulanova[1], Stanislav Petrov[1], Anna Gryadunova[1], Oleg Petrov[2], Mikhail Vasiliev[2], Maxim Myasnikov[2], Kenn Brakke[3], Domingues M. Carlos[4], Lorenzo Moroni[4], Yusef Khesuani[1], Vladimir Mironov[1]

[1] *Laboratory for Biotechnological Research "3D Bioprinting Solutions", Moscow, Russia;*

[2] *Joint Institute for High Temperatures, Russian Academy of Sciences, Moscow, Russia;*

[3] *Susquehanna University, Selinsgrove, Pennsylvania 17870,USA;*

[4] *Maastricht University, The Netherland.*

vapar@mail.ru

Introduction: Tissue spheroids have been proposed as building blocks in 3D spheroids-based biofabrication [1]. Magnetic forces-driven 2D patterning of tissue spheroids requires cell labelling by magnetic nanoparticles [2]. Label-free approach for magnetic levitation has been introduced recently for living cells [3]. Here we report for the time rapid assembly of 3D tissue construct using scaffold-free and label-free magnetic levitation of tissue spheroids in high magnetic field.

Methods: Tissue spheroids of standard size, shape and capable to tissue fusion have been biofabricated using non-adhesive technology. Label-free magnetic levitation has been performed using experimental device with permanent magnets and bitter electromagnet in presence of gadolinium in culture media, which enables magnetic levitation. Potential toxic effects of gadolinium have been systematically evaluated in advance.

Mathematical modelling and MD simulation of dynamics [4] have been used for prediction of magnetic field (Fig. 1a), forms (Fig. 1b), kinetics of tissue spheroids assembly into 3D tissue constructs (Fig. 1c), and simulation formation of cavity and empty spaces between tissue spheroid as result of their incomplete fusion.

Results: First of all polysterene beads were used as analogs of tissue spheroids for determination of an optimal settings for magnetic levitation in presence of gadolinium. Second, it has been shown that tissue spheroids were able to assemble rapidly into 3D tissue construct in the permanent nonhomogeneous magnetic field in the presence of gadolinium. Thus, label-free magnetic levitation of tissue spheroids is a promising approach for rapid scaffold-free 3D biofabrication and attractive alternative to label-based magnetic forces-driven tissue engineering. Scanning electron microscopy clearly demonstrated the fusion of tissue spheroids in 3D tissue construct (Fig.1d).

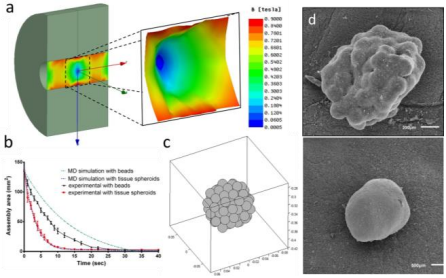

Fig. 1. (a) The nonhomogeneous static magnetic field generated by the magnetic setup. (b) - The kinetics of simulated and experimental construct assembly from polystyrene beads and chondroshperes. (c) MD simulation of the chondrospheres dynamics in the cusp magnetic trap. (d) Scanning electron microscopy image of chondrosheres construct and mouse thyroid gland construct assembled in a magnetic field during 24 hours.

Conclusions: Magnetic force provides a unique opportunity to levitate an assembly of tissue spheroids or more sophisticated structures in a culture medium. The results obtained in this study demonstrate that the magnetic field can be effectively used for scaffold-free and label-free magnetic levitational assembly of tissue spheroids in non-toxic concentration $Gd3^+$ paramagnetic medium. The combination of acoustic and magnetic fields can later give tremendous effect in the creation of tissue constructs.

We acknowledge the support of the HFML, member of the European Magnetic Field Laboratory (EMFL)

References:

[1] V. Mironov et al, Biomaterials.2009; 12, 2164.
[2] B. Whatley et al, J. Biomed. Mater. Res A.2014; 102,1537.
[3] A. Tocchio et al, Adv. Materials. 2017, 1705034.
[4] M.I. Myasnikov et al, J. of Experimental and Theoretical Physics 124, No. 2, 318.

Poster-Mo28

Non-Markovian memory effects explored with 2DFT spectroscopy at high magnetic fields

C. E. Stevens,[1] J. Paul,[1] V. Mapara,[1] J. L. Reno,[2] S. A. McGill,[3] V. Turkowski,[4] M. D. Kapetanakis,[5] I. E. Perakis,[5] D. J. Hilton,[5] and D. Karaiskaj[1]

[1] *Department of Physics, University of South Florida, Tampa, Florida 33620, USA*

[2] *CINT, Sandia National Laboratories, Albuquerque, New Mexico 87185, USA*

[3] *National High Magnetic Field Laboratory, Florida State University, Tallahassee, FL 30201, USA*

[4] *Department of Physics, University of Central Florida, Orlando, Florida 32816, USA*

[5] *Department of Physics, University of Alabama at Birmingham, Birmingham, Alabama 35294, USA*

In a time-integrated four-wave mixing (FWM) experiment the three pulses A*, B, and C are sent to the sample separated by the time delays τ and T. The pulse sequence is varied from *negative* delays, where the conjugate pulse A* trails behind B and C (Fig. 1 (b)) to *positive* delay where A* arrives ahead of B and C (Fig. 1 (a)). The time-integrated FWM signal in the negative time-delay regime is the most striking signature of the difference between nonlinear optical response of a collection of atoms and a solid state. This seemingly counterintuitive behavior that appears to violate causality is a result of the Coulomb interactions, which are dominant in semiconductors.

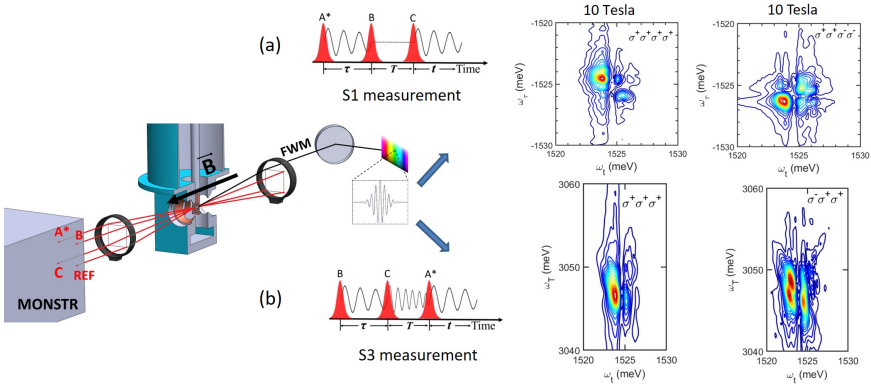

FIG. 1. *Schematic of the experimental setup: The four phase-stabilized laser beams are provided by the MONSTR instrument. Three beams labeled as A*, B, and C are used to generate the FWM signal, where A* corresponds to the phase conjugate beam. A fourth beam labeled as Ref. is used as the local oscillator for heterodyne detection. The sample is a 200 nm thick bulk GaAs crystal kept at 1.6 Kelvin. The magnetic fields up to 10 Tesla are applied perpendicular to the sample surface. 2DFT spectra based on the S1 (positive delay) and S3 (negative delay) techniques at select polarizations are shown in (a) and (b), respectively.*

Bulk GaAs at high magnetic fields results in a complex and interesting behavior. The negative delay signal has been shown to increase very rapidly with increasing magnetic fields at low temperatures, eventually decaying at the same rate as the positive delay signal. Furthermore, the negative delay displayed a non-exponential decay indicating non-Markovian memory effects [1]. Two-dimensional Fourier transform spectroscopy (2DFT) based on the FWM signal has been proven as an excellent tool which can provide deeper insights, revealing quantum coherent coupling [2] and many-body interactions [3]. We perform 2DFT measurement at select polarizations and on bulk GaAs at magnetic fields up to 10 Tesla. Two 2DFT configurations labeled as S1 and S3 in Fig. 1 (a) and (b) are used, based on the positive and negative delay FWM signals, respectively. These measurements combined with theoretical calculations provide important details on the underlying physics taking place.

[1]D. S. Chemla and J. Shah, Nature **411**, 549 (2001)
[2]J. Paul *et al.* Phys. Rev. Lett, **116**, 157401 (2016)
[3]J. Paul *et al.* Phys. Rev. B, **95**, 245314 (2017)

Poster-Mo29

Electronic properties of mixed Lead - Tin hybrid perovskites studied via magneto - spectroscopy

Krzysztof Galkowski,[1,2,3] Alessandro Surrente,[1] Michal Baranowski,[1] Baodan Zhao,[2] Aditya Sadhanala,[2] Sebastian Mackowski,[3] Samuel D. Stranks,[2] and Paulina Plochocka[1]

[1] *Laboratoire National des Champs Magnétiques Intenses, CNRS-UGA-UPS-INSA, Toulouse, France*

[2] *Cavendish Laboratory, University of Cambridge, JJ Thompson Avenue, Cambridge CB3 0HE, UK*

[3] *Institute of Physics, Faculty of Physics, Astronomy and Informatics, Nicolaus Copernicus University, 5th Grudziadzka St., 87-100 Toruń, Poland*

The exceptionally rapid growth of power conversion efficiency of photovoltaic cells based on the family of organo-lead halide perovskites has recently halted at around 20-22%. Among the limiting factors are relatively high band gaps (> 1.5 eV) of these materials, hampering the harvested part of the solar spectrum. As a promising perspective for pushing the performance towards new records, tandem perovskite-perovskite solar cells have been proposed, with low band-gap (> 1.2 eV) Lead-Tin (Pb:Sn) hybrid perovskite alloys used to fabricate the bottom cell [1].

However, the Pb:Sn perovskite compounds are yet on relatively early stage of the development, thus the number of reports concerning their fundamental electronic properties is limited. It has been proved, that high field pulsed magneto-spectroscopy provides a direct way to measure two of the most important electronic parameters - the binding energy of the exciton (R*) and its reduced effective mass (μ) [2,3].

In this work we present magneto-optical studies of Methylammonium (MA) Triiodide family with varying Lead-Tin composition ($MAPb_xSn_{1-x}I_3$; $x = 0.0, 0.2, 0.4, 0.6, 0.8, 1.0$) [4]. We fit the excitonic states as a hydrogenic atom in magnetic field and also observe Landau levels for free carriers to give R* and μ (Figure 1). We show that R* remains of the order of 15 meV; such a small value is in agreement with results obtained in our previous studies of other hybrid [3] and fully inorganic [5] perovskite tri-iodides. Furthermore, we observe that μ slowly follows the material band gap. This behaviour, reported for a range of different ionic compositions [3,5], can be generalized to all perovskite absorbers.

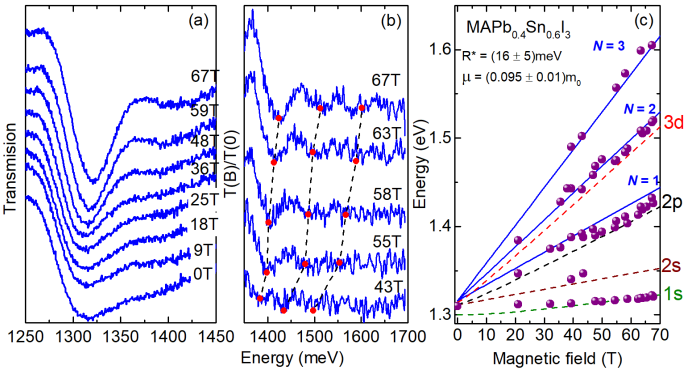

FIG. 1. *Magneto transmission results on $MAPb_{0.4}Sn_{0.6}I_3$: (a) transmission spectra and (b) differential transmission spectra $T(B)/T(0)$ in magnetic fields showing absorption of 1s excitonic state and higher free carrier transitions, respectively. (c) Energies obtained from the experimental data and results of the fit to the data. The results of the theoretical fit are presented by color dash (hydrogenic atom) and blue solid (free carrier) lines.*

[1]G.E. Eperon *et al.* Science, **20**, (2016)
[2]A. Miyata *et al.* Nature Physics **11**, 582587 (2015)
[3] K. Galkowski *et al.*, Energy & Environmental Science **9**, 962-970 (2016)
[4] B. Zhao *et al.*, Adv.Mater. **29**, 1604744 (2017)
[5] Z. Yang *et al.*, ACS Energy Letters **7**, 1621-1627 (2017)

Poster-Mo30

Anomalous Hall effect in metals with weak disorder

I.A. Ado,[1] I.A. Dmitriev,[2,3,4] P. M. Ostrovsky,[3,5] and M. Titov[1,6]

[1] *Radboud University, NL-6525 AJ Nijmegen, The Netherlands*

[2] *University of Regensburg, 93040 Regensburg, Germany*

[3] *Max Planck Institute for Solid State Research, 70569 Stuttgart, Germany*

[4] *A. F. Ioffe Physico-Technical Institute, 194021 St. Petersburg, Russia*

[5] *L. D. Landau Institute for Theoretical Physics RAS, 119334 Moscow, Russia*

[6] *ITMO University, Saint Petersburg 197101, Russia*

We demonstrate [1-3] an important role of quantum interference of scattering on pairs of close weak impurities in the theory of anomalous Hall effect (AHE). For weak scalar impurities, the differential cross-section in the leading order (Born approximation) is always symmetric with respect to the scattering angle. Therefore, in the standard limit of weak scalar Gaussian disorder, the skew-scattering contribution to the AHE appears due to pairs of impurities separated by a short distance of the order of the Fermi wave length. This makes necessary a complete treatment of scattering on such complexes including quantum interference effects.

Analytic calculations for two basic models of AHE demonstrate that account for the quantum interference qualitatively modifies previous results for the anomalous Hall conductivity. In particular, for massive Dirac fermions subject to a weak white-noise Gaussian disorder, the quantum interference parametrically suppresses the Hall conductivity [1]. By contrast, in the Bychkov-Rashba model the anomalous Hall conductivity does not vanish solely due to the interference contributions [2]. Therefore, we show that the well-known full cancellation of the intrinsic, side-jump, and skew-skattering contributions in this basic model of AHE is actually an artefact of incomplete treatments missing the quantum interference effects.

In Ref. [3] we demonstrate that AHE is highly sensitive to the correlation properties of weak disorder despite being independent of the integral disorder stength. In particular, for massive Dirac fermions the AHE is parametrically enhanced in the limit of small-angle scattering (corresponding to a weak Gaussian disorder with large correlation length) as compared to the case of white noise disorder [1] (the limit of small correlation length).

I.A.D. gratefully acknowledges the support from the Deutsche Forschungsgemeinschaft (Project No. DM 1/4-1).

[1] I.A. Ado *et al.*, EPL **111**, 37004 (2015).

[2] I.A. Ado *et al.*, Phys. Rev. Lett. **117**, 046601 (2016).

[3] I.A. Ado *et al.*, Phys. Rev. B **96**, 235148 (2017).

Hall electric field activated resistivity and the breakdown of the quantum Hall effect in GaAs and graphene

J. Huang and R.J. Nicholas
Department of Physics, University of Oxford, Clarendon Laboratory, Parks Road, Oxford OX1 3PU, UK
r.nicholas1@physics.ox.ac.uk

A number of reports[1-3] have previously shown that the resistivity minima at the quantum Hall condition show electric field dependence of the activated conduction which are given by the equations: $\rho_{xx} = \rho_0 \exp(-E_A/kT)$ and $E_A = \Delta_0 - eaE_H$, where a is thought to be associated with an activation length and E_H is the Hall electric field. To date the explanation of this behavior is uncertain. Here we demonstrate that this behavior occurs in typical GaAs/GaAlAs heterojunctions as used for standards applications and explore the highly asymmetric conduction and breakdown behavior for different regions of the resistivity minimum.

We investigate the dependence of the conductivity on Hall field, temperature and magnetic field close to the $\nu = 2$ minimum in a variety of Hall bars of different widths. We show that the localization lengths exhibit highly asymmetric behavior for conduction dominated by the $N = 0$ or $N = 1$ Landau levels, with localization lengths much shorter when the chemical potential is closest to the $N = 0$ level and that this behavior is most pronounced in a narrow Hall bar. Beyond the Hall field activated region there is a sudden increase in resistivity at current densities attributable to the quantum Hall breakdown region. This behavior persists well beyond the resistivity minimum and the resistivity displays a well pronounced negative differential resistance even up to temperatures as high as 15 K. These results suggest that around the critical breakdown current regime there is a dramatic change in the conduction process under a variety of different parameters.

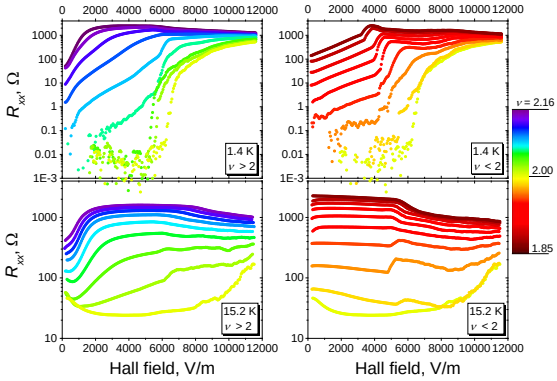

FIG. 1. Resisitivity of the $\nu = 2$ minimum as a function of the Hall electric field for a set of occupancies around the minimum value for a GaAs/GaAlAs heterojunction in the magnetic field range of 9.5–11.2 T.

We have also studied the same behavior in low density epitaxial graphene samples where the chemical potential lies close to the Dirac point, which are good candidates for new resistance standards[4]. The graphene shows similar activation behavior with a very similar activation length of order 300 nm, comparable to typical length scales determined from potential profiling.

References

[1] S. Komiyama *et al.* Solid State Commun. **54** 479 (1985).
[2] A. Boisen *et al.*, Phys. Rev. B **50**, 1957 (1994).
[3] T. Shimada *et al.* Physica B: Condensed Matter **249-251** 107 (1998).
[4] A.M.R. Baker et al. Phys. Rev. B **87**, 045414 (2013).

Poster-Mo32

Nonlinear dynamics, noise-induced reversals, and self-oscillations of electric field domains in the microwave-induced zero resistance states

I.A. Dmitriev[1, 2, 3]

[1] *University of Regensburg, 93040 Regensburg, Germany*

[2] *Max Planck Institute for Solid State Research, 70569 Stuttgart, Germany*

[3] *A. F. Ioffe Physico-Technical Institute, 194021 St. Petersburg, Russia*

Discovery [1] of the zero resistance state (ZRS) in 2D electron systems subject to microwave radiation and weakly quantizing magnetic field attracted a great deal of attention and initiated intensive experimental and theoretical work that has greatly advanced the understanding of the physics of nonequilibrium phenomena in high Landau levels [2]. At the same time, understanding of ZRS itself, especially of the structure and dynamics of electrical domains in ZRS, remains limited. In particular, while theory [3] predicts the emergence of static domains, recent experiments [4-6] demonstrate a robust switching behavior, characterized by synchronous and almost periodic reversal of the domain field in the whole structure in time.

We propose a basic explanation of this behavior which agrees well with the available experimental findings [4-6]. The explanation is based on the presence of a parallel weakly conducting layer (passive layer) in close proximity to the high-mobility 2D electron system (active layer) driven into ZRS . In real structures, such passive layer is formed by electrons in the X-valleys of AlAs barriers surrounding narrow highly doped GaAs quantum wells at a typical distance about 50 nm from the active layer. Due to its low conductivity, the passive layer is almost insensitive to both the applied magnetic field and the microwave illumination. At the same time, a (delayed) screening of the spontaneous electric field in domains by electrons in the passive layer dramatically changes the picture of ZRS.

The analysis of a basic theoretical model of ZRS in such two-layer system demonstrates the emergence of a number of new static and dynamical regimes, including self-oscillations of the spontaneous domain field in the whole structure, as well as the noise-induced reversals which can be both enhanced and completely suppressed due to the presence of the passive layer. Estimates show that for parameters typical for present experiments, the passive layer facilitates the noise-induced transition to the state with the opposite polarity of the domain field, by dynamically lowering the barrier separating the two states. This explains the almost periodic switching observed in the experiments. The proposed explanation is strongly supported by recent measurements [6] which demonstrate the same activated temperature dependence for the passive layer conductivity and typical switching times of the domain field in ZRS for a given heterostructure, as well as by the observation [5] of transient self-oscillations of the domain field in the vicinity of transition to ZRS.

The support from the Deutsche Forschungsgemeinschaft (Project No. DM 1/4-1) is gratefully acknowledged.

[1] R.G. Mani *et al.*, Nature **420**, 646 (2002); M.A. Zudov *et al.*, Phys. Rev. Lett. **90**, 046807 (2003).

[2] I.A. Dmitriev *et al.*, Rev. Mod. Phys. **84**, 1709 (2012).

[3] A.V. Andreev, I. L. Aleiner, and A. J. Millis, Phys. Rev. Lett. **91**, 056803 (2003); A. Auerbach *et al.*, Phys. Rev. Lett. **94**, 196801 (2005); I.A. Dmitriev *et al.*, Phys. Rev. Lett. **111**, 206801 (2013).

[4] S.I. Dorozhkin *et al.*, Nature Physics **7**, 336 (2011); Phys. Rev. Lett. **114**, 176808 (2015); JETP Lett. **104**, 721 (2016).

[5] S.I. Dorozhkin, JETP Lett. **102**, 91 (2015).

[6] S.I. Dorozhkin *et al.*, JETP Lett. **107**, 61 (2018).

Poster-Mo33

Defect healing and inter-layer exciton in a CVD grown $MoS_2/MoSe_2/MoS_2$ heterostructure

A. Surrente,[1] M. Baranowski,[1] Ł. Kłopotowski,[2] N. Zhang,[3] J. Urban,[3] A. A. Mitioglu,[4] M. V. Ballottin,[4] P. C. M. Christianen,[4] D. Dumcenco,[5] Y.-C. Kung,[5] D. K. Maude,[3] A. Kis,[5] and P. Plochocka[3]

[1] *Laboratoire National des Champs Magnétiques Intenses, CNRS-UGA-UPS-INSA, Toulouse, France*

[2] *Institute of Physics, Polish Academy of Sciences, Al. Lotników 32/46, 02-668 Warsaw, Poland*

[3] *Laboratoire National des Champs Magnétiques Intenses, UPR 3228, CNRS-UGA-UPS-INSA, Grenoble and Toulouse, France*

[4] *High Field Magnet Laboratory (HFML – EMFL), Radboud University, 6525 ED Nijmegen, The Netherlands*

[5] *Electrical Engineering Institute and Institute of Materials Science and Engineering, École Polytechnique Fédérale de Lausanne, CH-1015 Lausanne, Switzerland*

Chemical vapour deposition (CVD) is a scalable growth technique which is extremely promising for the fabrication of large area transition metal dichalcogenides (TMD) monolayers. CVD grown TMDs are generally characterized by poor optical quality with broad photoluminescence (PL) emission dominated by defect bound excitons at cryogenic temperatures. Here we demonstrate that a simple fabrication approach, based on double-sided encapsulation of a CVD-grown $MoSe_2$ monolayer via transfer of CVD-grown MoS_2 flakes completely suppresses the defect-related emission, restoring the excellent optical quality of the sandwiched $MoSe_2$ layer. The low temperature PL emission of the encapsulated $MoSe_2$ monolayer exhibits a line-width comparable to that of mechanically exfoliated $MoSe_2$ (see Fig. 1(a)). This is consistent with a defect healing scenario, suggested by density functional theory, which predicts that it is energetically favourable for the more reactive MoS_2 to donate a chalcogen atom to fill Se vacancies in the encapsulated $MoSe_2$ [1]. The $MoS_2/MoSe_2$ heterostructure has a type-II band alignment. The charge transfer process after the initial photoexcitation is spin conserving, allowing us to observe for the first time a significant valley polarization of the $MoSe_2$ emission while exciting in resonance with the A exciton of MoS_2 X_A [1] (see inset of Fig. 1(a)). The interlayer nature of the low energy peak in Fig. 1(a) is confirmed by the sublinear dependence on the excitation power, the slow recombination dynamics with characteristic lifetimes of nanoseconds, and the non-monotonic temperature dependence of the peak intensity. Intriguingly, the interlayer exciton emission is counter-polarized with respect to the circularly polarized excitation [2]. The interlayer exciton emission in magnetic fields up to 28T (see Fig. 1(b)) shows a giant valley Zeeman splitting, yielding an effective g-factor of -13.1, as shown in Fig. 1(c-d) which suggests a stacking angle of 60° between the optically active monolayers [3]. The large Zeeman splitting allows us to manipulate the valley polarization, which can be tuned controllably up to almost 100%, as summarized in Fig. 1(d). The magnetic field dependence of the valley polarization can be explained using a simple rate equation model, which accounts for inter-valley scattering processes such as valley depolarization via electron-hole exchange interaction and one-phonon spin-lattice relaxation [4].

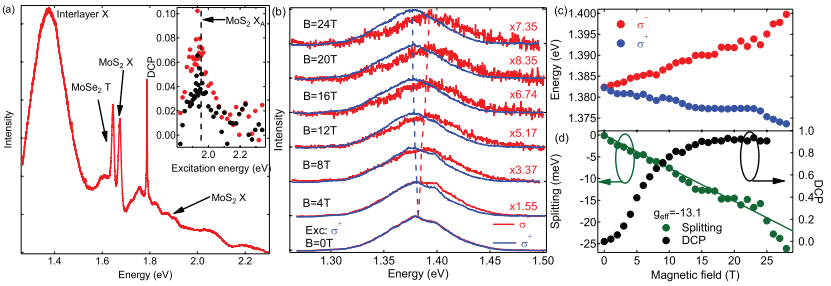

FIG. 1. *(a) Low temperature μPL spectrum of a $MoS_2/MoSe_2/MoS_2$ trilayer. Inset: DCP of $MoSe_2$ X and T versus excitation energy. The dahsed line indicates the energy of X_A in MoS_2. (b) Interlayer exciton magnetoPL spectra up to 24T. The spectra detected with σ_- polarization have been rescaled for clarity. (c) Transition energies, (d) energy splitting and DCP of interlayer exciton as a function of magnetic field.*

[1] A. Surrente, *et al.*, Nano Letters **17**, 4130 (2017) [2] M. Baranowski, A. Surrente, *et al.*, Nano Letters **17**, 6360 (2017) [3] P. Nagler, *et al.*, Nature Communications **8**, 1551 (2018) [4] A. Surrente, *et al.*, submitted

Poster-Mo34

Variable range hopping conduction and magnetoresistance in ordered defect compounds.

L. Essaleh [1], S. M. Wasim [2], G. Marín [3], C. Rincón [2], S. Amhil [1], J. Galibert [4]

[1] *Laboratory of Condensed Matter and Nanostructures (LMCN), Cadi-Ayyad University, Faculty of Sciences and Technology, Department of Applied Physics, Marrakech, Morocco.*

[2] *Centro de Estudios de Semiconductores, Facultad de Ciencias. Universidad de Los Andes, Mérida 5101, Venezuela.*

[3] *Laboratorio de Estructura e Ingeniería de Materiales Nanoestructurados (LEIMN), Centro de Investigación y Tecnología de Materiales (CITeMa), InstitutoVenezolano de InvestigacionesCientíficas (IVIC), Maracaibo 4011, Venezuela.*

[4] *Laboratoire National des Champs Magnétiques Intenses, LNCMI-EMFL, CNRS/INSA/UGA/UPS, Toulouse & Grenoble, France.*

Some members, like $Cu(In,Ga)Se_2$, of Cu-ternaries of the I-III-VI_2 family are being employed in the fabrication of photovoltaic devices. Others, that are also expected to play important role, belong to Cu-III_3-VI_5 family. These compounds, that are formed on the In-rich side of the pseudo-binary phase diagram of $(Cu_2Se)_{1-x}$-$(In_2Se_3)_x$ have a deficiency of one cation over the anions. These ordered Defect Compounds (ODCs) were initially referred to as Ordered Vacancy Coupounds (OVCs).
We will report, in the present paper, on the electrical resistivity in a wide temperature range to establish the type of conduction mechanism and also the variation of magnetoresistance (MR) up to 30 T at different temperatures for some representative ODC compounds. The results are analysed and compared with the existing theoretical models.

In p type $CuGa_3Te_5$ **[1]** variable range hopping conduction (VRH) of Efros-Shklovskii type (ES) for a vanishing density of states, when a Coulomb gap due to repulsive interaction of free carriers appears at the Fermi level, is observed in the temperature range [4-150 K]. This type of electrical conduction over such a wide temperature range is possibly due to very low concentration of charge carriers as compared to the critical concentration Nc that defines the Mott's metal-insulator transition (MIT). The MR is positive over the whole magnetic field range and between 4 and 40 K. Its behaviour both at low and high field up to 30 T is analysed in the framework of the ES theoretical model for VRH. To our knowledge this study is the only work where the proposed model for the variation of MR when the conduction is of a ES-VRH type, is confirmed. This has not been reported in either I-III-VI_2 or any other I-III_3-VI_5 compounds.

In n-$CuIn_3Se_5$ **[2]**, VRH of Mott type is observed in two different temperature range between 10K and 65K.
In p-$CuIn_3Te_5$ **[3],** another ODC of the I-III_3-VI_5 family, Mott type of VRH conduction is observed in wide temperature range [45-210 K]. Negative magnetoresistance (NMR) at low fields is observed, and is explained to be due to the quantum interferences between many path connecting impurity sites during the hopping process *(model of N'Guyen, Spivak & Shklovskii-NSS-***[4]***)*. The variation of magnetoresistance (MR) at higher fields at different temperatures, is explained with the theoretical model for Mott-type VRH. To our knowledge, this study is the only work where the proposed model for the variation of MR when VRH is of Mott type is confirmed over a wide temperature range up to 210 K in ODCs.

[1] S.M Wasim, L. Essaleh, G. Marín, C. Rincón, S. Amhil, J. Galibert Superlattices and Microstructures 107, 285 (2017)
[2] S.M. Wasim, L. Essaleh, G. Marín, J. Galibert Materials Research Bulletin 87, 219 (2017)
[3] L. Essaleh, S.M. Wasim, G. Marín, C. Rincón, S. Amhil, J. Galibert J. Applied Physics 122, 015702 (2017)
[4] V. L. Nguyen, B. A. Spivak, B. I. Shklovskii, Sov. Phys. JETP**62**, 1021 (1985); Sov. Phys. JETP Lett.**41**, 42 (1985).

Poster-Mo35

Inter-edge electron transport in Corbino topology in Quantum Hall Regime

A. Delgard,[1] B. Chenaud,[1] C. Chaubet,[1] U. Gennser,[2] D. Mailly,[2] K. Ikushima,[3] and S. Okano[3]

[1] *Laboratoire Charles Coulomb, CNRS-Universit Montpellier, Montpellier, France*

[2] *Centre de Nanosciences et de Nanotechnologie, CNRS, Marcoussis, France*

[3] *Department of Applied Physics, Tokyo University of Agriculture and Technology, Koganei, Tokyo, Japan*

In Quantum Hall regime, electron drives along edge channel which contribu. Each edge-state contributes to bar conductance with $\frac{e^2}{h}$[1], [2]. This property has two consequences: first, Hall resistance is quantized (thereby Quantum Hall effect is used as the Ohm unit standard[3]), second, the longitudinal resistance in Quantum Hall regime is zero. Thus, an edge state is a perfect conductor, a ballistic electron highway.[4].

In Corbino topology, electron transport is different. Edge-states turn around the voltage contact and don't cross the ring[5]. The conductance of the Corbino is theoretically vanishing, however, we measure resistance from 10 $M\Omega$ to 1 $G\Omega$.

We study the effect of bias voltage on this Corbino resistance. We measure in fact the interedge scattering and observe the robustness of the edge transport in this regime. We can observe in this topology the premisses of Quantum Hall breakdown, its initiation by hopping process[6],[7]. We also perform measurement for different temperatures which is another parameter to induce this electron avalanche.

Another way to measure this transition effect is to measure our sample in AC regime. In this regime, a Corbino is is described by a quantum capacitance[8]. The existence of the quantum capacitance guarantee the existence of the edge channel so it's a good way to measure their robustness. That's why we study variation of the Corbino capacitance with bias voltage and temperature.

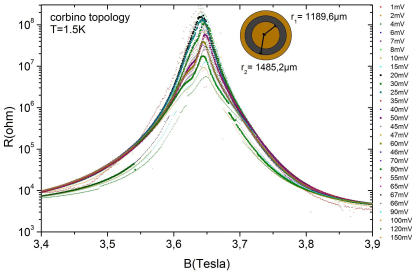

FIG. 1. *Bias voltage dependance of Corbino longitudinal resistance in Quantum Hall regime (filling factor $\nu = 2$)*

[1] K. von Klitzing *et al.*, Phys. Rev. Lett. 45, 494 (1980)

[2] D. C. Tsui *et al.* Phys. Rev. Lett., 1559 **48**, (1982)

[3] Comité International des Poids et Mesures, Recommandation 2 (CI-1991) 19th CGPM (1991)

[4] Buttiker *et al.* Phys. Rev. Lett., textbf57 17611764 (1986)

[5] B. Jeanneret *et al.* IEEE Transactions on Instrumentation and Measurement, **48** 301 - 304, (1999)

[6] G. Nachtwei Physica E, **4** 79-101 (1999)

[7] C. Chaubet *et al.* Semiconductor Science And Technology, vol. 18 p.983-991 (2003)

[8] Buttiker *et al.* Phys. Rev. B 53, 2064 (1996).

Poster-Mo36

A new 2D material for hydrogen storage application

M. Garara [a,*], H. Benzidi [a], M. Lakhal [a], M. Louilidi [a], A. El kenz [a], M. Hamedoun [b], A. Benyoussef [b], A. Kara [c] and O. Mounkachi [a,b]

a Laboratory of Condensed Matter and Interdisciplinary Sciences, Physics department, Faculty of Sciences, Mohammed V University, Rabat, Morocco

b Materials and Nanomaterials Center, MAScIR Foundation, Rabat Design Center Rue Mohamed Al Jazouli Madinat Al Irfane Rabat 10 100 Morocco

c Departement of Physics, University of Central Florida, Orlando, Florida 32816, United States

e-mail: garara.mourad@gmail.com

Phosphorene has become one of the most promising 2D materials, with properties that exceeded graphene. In this paper, the density functional theory was initially applied to stimulate the influence of hydrogen adsorption on the electronic and structural characteristics of phosphorene. Our calculations have been performed taking account the van der Waals interactions using the DF2-vdW method. Several adsorption sites and orientations of the hydrogen molecule relative to the phosphorus surface were considered and the associated binding energies and adsorption potential were computed. The analysis of diffusion pathways between different physisorbed states on phosphorene shows that molecular hydrogen can easily diffuse at room temperature from one configuration to another. the potential energy surfaces for the dissociative chemisorption of H2 was computed on highly symmetric sites of phosphorene. The barriers for H2 diffusion and dissociation on the phosphorene surface are significantly lowered with respect to the graphene case, showing the remarkable effect of the substrate curvature in promoting hydrogen dissociation and diffusion.

[1] L. Schlapbach and A. Züttel, “Hydrogen-storage materials for mobile applications.”,Nature, vol. 414, no. 6861, pp. 353–358, 2001.
[2] R. Roszak, L. Firlej, S. Roszak, P. Pfeifer, and B. Kuchta, “Hydrogen storage by adsorption in porous materials: Is it possible?” Colloids and Surfaces A: Physicochemical and Engineering Aspects, Elsevier B.V., 2015.
[3] S. Satyapal, J. Petrovic, C. Read, G. Thomas, and G. Ordaz, “The U.S. Department of Energy’s National Hydrogen Storage Project: Progress towards meeting hydrogen-powered vehicle requirements,” Catal. Today, vol. 120, no. 3–4 SPEC. ISS., pp. 246–256, 2007.
[4] T. F. and F. Partnership, “Targets for onboard hydrogen storage systems for light duty vehicles”,US Dep. Energy, no. September, pp. 1–22, 2009.
[5] M. Yoon, S. Yang, E. Wang, and Z. Zheng, “Charged fullerenes as high-capacity hydrogen storage media,” Nano Lett., vol. 7, no. 9, pp. 2578–2583, 2007.
[6] S. Orimo, Y. Nakamori, J. R. Eliseo, A. Züttel, and C. M. Jensen, “Complex Hydrides for Hydrogen Storage,” Chem. Rev., vol. 107, no. 10, pp. 4111–4132, 2007.
[7] Z. Wu, L. Chen, X. Xiao, X. Fan, S. Li, and Q. Wang, “Influence of lanthanon hydride catalysts on hydrogen storage properties of sodium alanates,” J. Rare Earths, vol. 31, no. 5, pp. 502–506, 2013.
[8] V. Tozzini and V. Pellegrini, “Prospects for hydrogen storage in graphene,” Phys. Chem. Chem. Phys., vol. 15, no. 1, pp. 80–89, 2013.
[9] E. Yoo, J. Kim, E. Hosono, H. Zhou, T. Kudo, and I. Honma, “Large Reversible Li Storage of Graphene Nanosheet Families for Use in Rechargeable Lithium Ion Batteries 2008,” pp. 13–18, 2008.
[10] Y. Miura, H. Kasai, W. Diño, H. Nakanishi, and T. Sugimoto, “First principles studies for the dissociative adsorption of H2 on graphene,” J. Appl. Phys., vol. 93, no. 6, pp. 3395–3400, 2003.

	Sunday 22 July	Monday 23 July	Tuesday 24 July	Wednesday 25 July	Thursday 26 July	Friday 27 July
8h50		Opening				
9h00		P. Kim	N. Hussey	M. Yankowitz	T. Heinz	B. Béri
9h30		T. Szkopek	L.E. Golub	C. Dean	A. Arora	Lyand-Geller
9h45		M.V.Durnev	T. Khouri	L.Lzulakowska	J. Holler	F.Appugliese
10h00		J. Lau	D. Smirnov	B.Urbaszek	A. Mitioglu	S. Chen
10h15		E. Henriksen	S.Wiedmann	M.R. Molas	Slobodeniuk	M. Novak
10h30		Coffee break				
11h00		A. Young	A. Coldea	N. Wang	G. Gusev	L. Weiss
11h30		Y. Zhang	P. Sessi	M. Glazov	A. Suslov	O.Makarovsky
1200		Buffet Lunch	Buffet Lunch	Conference Excursion with packed lunch	Buffet Lunch	Closing
14h00		G. Yusa	R.McDonald		A. Surrente	
14h30		B. Fauqué	T. Story		A. Akrap	
15h00		T. Taen	K.S.Denisov		M. Naumann	
15h15		N. Han Tu	F. Telesio		Shahrokhvand	
15h30		X. Liu	K. Rubi		D.K. Efetov	
15h45		S. Crooker	R.Masutomi		F.Parmentier	
16h00		Coffee	Coffee		Coffee	
16h30		Shot gun 1 + Poster Session Mo + Cocktail dinatoire	Shot gun 2 + Poster Session Tu + Cocktail dinatoire		A.Gorbunov	
16h45					J. Oswald	
17h00					V.Gavrilenko	
17h15					M. Zudov	
17h30						
18h00	Welcome reception NOVOTEL					
20h00				Reception/ Banquet		
21h00						